

# **STUDY OF CHARACTERISATION AND PROPERTIES EVALUATION OF SOME AUTOMOBILE COMPONENTS**

A THESIS REPORT

SUBMITTED TO THE FACULTY OF ENGINEERING & TECHNOLOGY

JADAVPUR UNIVERSITY

IN PARTIAL FULFILMENT OF THE REQUIREMENTS FOR THE AWARD OF  
THE DEGREE OF

**MASTER OF ENGINEERING**

IN

INDUSTRIAL METALLURGY

By

***SUBHASISH SARKAR***

[Examination Roll No M4MET1603]

[Registration No 99598 of 07-08]

Under the Guidance of

**PROF.SHIDDHARTHA MUKHERJEE**

**DEPARTMENT OF METALLURGICAL AND MATERIAL ENGINEERING  
FACULTY OF ENGINEERING AND TECHGNOLOGY  
JADAVPUR UNIVERSITY**

**Kolkata-700032**

**INDIA**

**2016**

## Declaration of Originality and Compliance of Academic Ethics

---

I hereby declare that this thesis contains literature survey and original research work by the undersigned candidate, as part of his Master of Metallurgical Engineering in industrial Metallurgy faculty of Engineering and Technology, Jadavpur University, Session: 2015-2016 studies.

All information in this document have been obtained and presented in accordance with academic rules and ethical conduct.

I also declare that, as required by these rules and conduct, I have fully cited and Referenced all material and results that are not original to this work.

Name: Subhasish Sarkar

Roll Number: M4MET1603

Registration Number: 99598 of 07-08

**Thesis Title: STUDY OF CHARACTERISATION AND PROPERTIES  
EVALUATION OF SOME AUTOMOBILE COMPONENTS .**

Signature with date:

.....

(SUBHASISH SARKAR)

Date: .....

## CERTIFICATE OF RECOMMENDATION

*I hereby recommend that the thesis prepared under my supervision by Subhasish Sarkar, entitled, “**STUDY OF CHARACTERISATION AND PROPERTIES EVALUATION OF SOME AUTOMOBILE COMPONENTS**” be accepted in partial fulfilment of the requirements for awarding the degree of Master of Metallurgical Engineering under Department of Metallurgical and Material Engineering of Jadavpur University.*

.....  
PROF. SIDDHARTHA MUKHERJEE  
Thesis Advisor  
Dept. of Metallurgical and Material Engineering  
Jadavpur University  
Kolkata

.....  
PROF. S BANDYOPADHYAY  
Dean  
Faculty of Engineering and Technology  
Jadavpur university  
Kolkata

.....  
DR. ASKAY KUMAR PARAMANIK  
Professor & Head  
Dept.of Metallurgical and material Engineering  
Jadavpur University  
Kolkata

# JADAVPUR UNIVERSITY

Kolkata-700032

---

## Certificate of Approval

The foregoing thesis, entitled as is hereby approved by the committee of final examination for evaluation of thesis as a creditable study of an engineering subject carried out and presented by Mr. **Subhasish Sarkar** (Examination Roll No.-M4MET1603;

Registration No 99598 of 07-08) in a manner satisfactory to warrant its acceptance as a requisite to the degree of Master of Metallurgical Engineering. It is understood that by this approval, the undersigned do not necessarily endorse or approve any statement made, opinion expressed or conclusion drawn therein, but approve the thesis only for the purpose for which it is submitted.

Committee of final examination for evaluation of thesis.

.....

.....

***DEDICATED***  
***TO MY BELOVED PARENTS***  
***WHO ARE MY SOURCE OF***  
***INSPIRATION***

# CONTENTS

CHAPTER	PAGE NO
<b>1. INTRODUCTION:</b>	<b>2</b>
<b>2. LITARATURE REVIEW:</b>	<b>4</b>
<b>2.1 Steel</b>	<b>4</b>
2.1.1 Definition	4
2.1.2 Classification of steel	4
<b>2.2 Heat Treatment Processing</b>	<b>5</b>
2.2.1 Spheroidizing	6
2.2.2 Full annealing	6
2.2.3 Process annealing	7
2.2.4 Isothermal annealing	7
2.2.5 Normalizing	7
2.2.6 Quenching	7
2.2.7 Quench and tempering	8
<b>2.3 Forming Technology</b>	<b>8</b>
2.3.1 Hot Deformation	8
2.3.2 Hot rolling	10
2.3.3 Extrusion	14

2.3.4 Wire Drawing	17
2.3.5 Forging	18
<b>3. EXPERIMENTAL PROCEDURE</b>	<b>21</b>
<b>3.1 Metallography</b>	<b>21</b>
3.1.1 Sample Preparation	21
3.1.2 Optical Microscopy	24
3.1.3 Scanning Electron Microscopy (SEM)	26
3.1.4 Vickers Macro hardness test	27
3.1.5 X-Ray Diffraction	29
<b>4. RESULTS &amp; DISCUSSION</b>	<b>35</b>
<b>4.1 Kick Start of a Bike</b>	<b>35</b>
4.1.1 Source	35
4.1.2 Chemical Composition	36
4.1.3 Optical Microscopy	37
4.1.4 SEM Analysis	39
4.1.5 Phase analysis by XRD	40
4.1.6 Vickers Hardness Testing	41
4.1.7 Tensile Testing of Material	41
<b>4.2 Lever Arm of a Bike</b>	<b>44</b>
4.2.1 source	44
4.2.2 Chemical composition	44
4.2.3 Optical microscopy	45
4.2.4 SEM Analysis	46
4.2.5 Phase analysis by XRD	47
4.2.6 Vickers Hardness Testing	47

<b>4.3.Chain of a Bike</b>	<b>48</b>
4.3.1 Source	48
4.3.2 Chemical composition	49
4.3.3 Optical Microscopy	49
4.3.4 SEM Analysis	51
4.3.5 Phase analysis by XRD	52
4.3.6 Vickers Hardness Testing	
<b>4.4 Analysis Spoke of a bike</b>	<b>54</b>
4.4.1 Source	54
4.4.2 Chemical Composition	54
4.4.3 Optical microscopy	56
4.4.4 SEM analysis	56
4.4.5 Phase analysis by XRD	58
4.4.6 Vickers Hardness Testing	58
<b>4.5 Clutch of a bike</b>	<b>59</b>
4.5.1 Source	59
4.5.2 Chemical Composition	59
4.5.3 Optical Microscopy	61
4.5. 4 SEM analysis	63
4.5.5 Phase analysis by XRD	64
4.5.6 Vickers Hardness Testing	65
<b>4.6 General Discussion</b>	<b>66</b>
<b>5. REFERCNCE</b>	<b>70</b>



## ABSTRACT

Different types of steels and cast iron are used by mechanical engineers in various automobile components. Some of the components have been collected and studied to evaluate their metallurgical quality.

The majority of the components were taken from transport sector starting with kick rod of a motor bike, lever arm of a bike, chain of a bike, clutch plate of a bike were tested and characterized using standard metallurgical tests such as- microstructural studies by optical microscopy, morphological analysis by SEM and evaluation of some mechanical properties.

Majority of the components produce acceptable metallurgical quality as most of the steels were produced by forging /rolling process.

Key Word:Microstructure,SEM,Hardness,XRD,Chemical composition(XRF),motorbike kick rod,chain,spoke,clutch plate

# CHAPTER 1

## INTRODUCTION

## INTRODUCTION

Indian manufacturing sector is getting boosted for developing new areas of automobile and other engineering industry. To provide leadership in those engineering Mechanical designers are taking keen interest in all kinds of new materials, in which steels and allied sections take prominent seat. In this respect it becomes quite natural to look at those ferrous metals from metallurgical perspective.

To explore the automobile and allied engineering areas of construction a few functional Iron-carbon alloys were collected from running units for investigation .All the materials were subjected to simple metallurgical characterization to evaluate their quality.

# **CHAPTER 2**

## **LITERATURE REVIEW**

## 2. LITERATURE REVIEW:

---

### 2.1 STEEL

#### 2.1.1 DEFINITION:

Steel is an alloy of iron & Carbon, with carbon may contribute maximum up to 2% with no primary carbide. Other residuals elements like Si, Mn and some minor inclusions may present. The alloying elements may be added to improve the properties of the steel.

#### 2.1.2 CLASSIFICATION OF STEEL

The carbon is the most important alloying element for commercial steel. Increasing carbon content increases hardness and strength and improves hardenability. But carbon also increases brittleness and reduces weldability because of its tendency to form martensite during quenching. This means carbon content can be both a blessing and a curse when it comes to commercial steel.

The steels are classified into three groups:

- A. Plain Carbon Steel
- B. Low-Alloy Steel
- C. High-Alloy Steel.

#### ➤ A. **Plain Carbon Steels:**

These steels usually are iron with less than 1 per cent carbon, plus small amounts of manganese and silicon with residual amount of P & S.

According to association of carbon percentages plain carbon steels are divided four groups.

1. Low (C < 0.30% known as Mild-Steel.)
2. Medium ( C- 0.30 to 0.45 % )
3. High ( C- 0.45 to 0.75 % )
4. Very high ( C up to 1.50 % )

➤ B. **Low-Alloy Steels:**

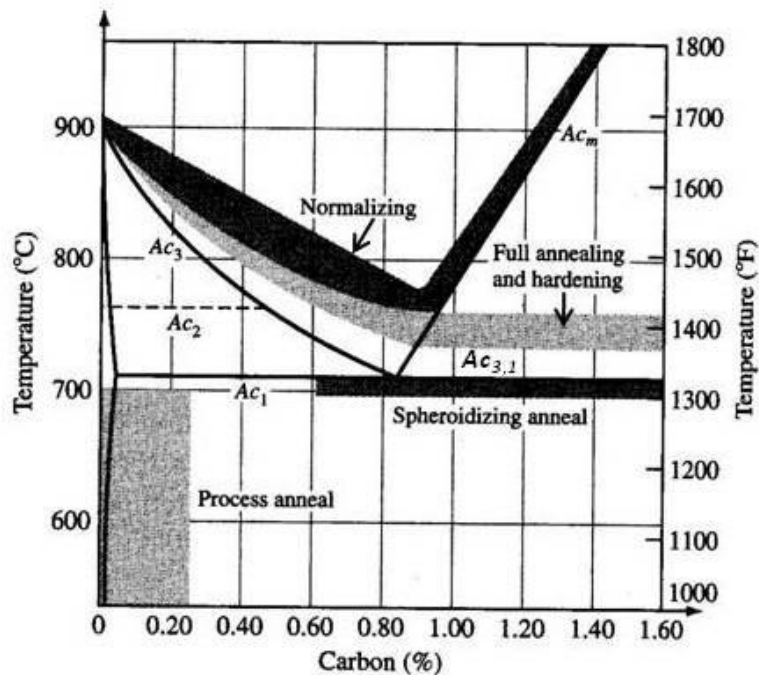
When these steels are designed for welded applications, their carbon content is usually below 0.25 per cent and often below 0.15 per cent. Typical alloys include nickel, chromium, molybdenum, manganese, vanadium, tungsten and silicon.

➤ C. **High-Alloy Steels:**

The most important commercial steel is high-alloy steel. Stainless steels are at least 12 per cent or more alloying elements like chromium, Nickel etc.

## **2.2 HEAT TREATMENT PROCESSING:**

Steels are among the relatively few engineering alloys which can be heat-treated in order to vary their mechanical properties. This statement refers, of course, to heat-treatments other than simple stress-relief annealing processes. Heat-treatments can be applied to steel not only to harden it but also to improve its strength, toughness or ductility. The type of heat treatment used will be governed by the carbon content of the steel and its subsequent application. In this process the steel is heated fairly slowly to some predetermined temperature, and then cooled, and it is the rate of cooling which determines the resultant structure of the steel and, hence, the mechanical properties associated with it.



Temperature Range for Heat Treatment of Carbon Steels

**2.2.1 Spheroidizing:** Spheroidite forms when carbon steel is heated to approximately 700°C for over 30 hours. Spheroidite can form at lower temperatures but the time needed drastically increases, as this is a diffusion-controlled process. The result is a structure of rods or spheres of cementite within primary structure (ferrite or pearlite, depending on which side of the eutectoid you are on). The purpose is to soften higher carbon steels and allow more formability. This is the softest and most ductile form of steel.

**2.2.2 Full annealing:** Carbon steel is heated to approximately 40 °C above  $Ac_3$  or  $Ac_1$  for 1 hour; this ensures all the ferrite transforms into austenite (although cementite might still exist if the carbon content is greater than the eutectoid). The steel must then be cooled slowly, in the realm of 20 °C (68 °F) per hour. Usually it is just furnace cooled, where the furnace is turned off with the steel still inside. This results in a coarse paralytic structure, which means the "bands" of pearlite are thick. Fully annealed steel is soft and ductile, with no internal stresses.

**2.2.3 Process annealing:** A process used to relieve stress in cold-worked carbon steel with less than 0.3 wt. % C. The steel is usually heated up to 550–650 °C for 1 hour, but sometimes temperatures as high as 700 °C. The image rightward shows the area where process annealing occurs.

**2.2.4 Isothermal annealing:** It is a process in which hypo eutectoid steel is heated above the upper critical temperature and this temperature is maintained for a time and then the temperature is brought down below lower critical temperature and is again maintained. Then finally it is cooled at room temperature. This method rids any temperature gradient.

**2.2.5 Normalizing:** Carbon steel is heated to approximately 55 °C above  $A_{c3}$  or  $A_{cm}$  for 1 hour; this ensures the steel completely transforms to austenite. The steel is then air-cooled, which is a cooling rate of approximately 38 °C (100 °F) per minute. This results in a fine paralytic structure, and a more-uniform structure. Normalized steel has a higher strength than annealed steel; it has a relatively high strength and ductility.

**2.2.6 Quenching:** Carbon steel with at least 0.4 wt% C is heated to normalizing temperatures and then rapidly cooled (quenched) in water, brine, or oil to the critical temperature. The critical temperature is dependent on the carbon content, but as a general rule is lower as the carbon content increases. This results in a martensitic structure; a form of steel that possesses a super-saturated carbon content in a deformed body-centred cubic (BCC) crystalline structure, properly termed body-centred tetragonal (BCT), with much internal stress. Thus quenched steel is extremely hard but brittle, usually too brittle for practical purposes. These internal



stresses cause stress cracks on the surface. Quenched steel is approximately three to four (with more carbon) fold harder than normalized steel.

**2.2.7 Quench and tempering:** This is the most common heat treatment encountered, because the final properties can be precisely determined by the temperature and time of the tempering. Tempering involves reheating quenched steel to a temperature below the eutectoid temperature then cooling. The elevated temperature allows very small amounts of spheroidite to form, which restores ductility, but reduces hardness. Actual temperatures and times are carefully chosen for each composition.

## 2.3 FORMING TECHNOLOGY

### 2.3.1 HOT DEFORMATION

#### Flowstresses

At homologous temperatures above  $0.4T_m$ , plastic deformation is strongly influenced by thermally activated processes so that the flow stress becomes temperature and strain rate dependent (viscoelastic). The processes involved are mostly controlled by local atomic diffusion and give rise to strong dynamic recovery of the dislocation substructure as the dislocations are continuously annihilated during deformation by climb and cross-slip mechanisms. This strongly reduces the flow stresses which then tend to saturate at values function of  $T$ , and alloy content. It is generally recognized that the  $T$  and terms can be regrouped into a temperature-compensated strain rate known as the Zener–Hollomon parameter

$$Z = \dot{\epsilon} \exp(Q/RT)$$

where  $R$  is the gas constant

$Q$  an apparent activation energy for plastic flow.

When atoms are added to the alloy,

the resistance to dislocation movement will increase and so does the value of  $Q$ . For the austenitic stainless steels, and also for many other low-or-medium fcc metals, the rate of dynamic recovery is limited even at elevated temperatures (the standard mechanism of annihilation by cross-slip is hampered by the inability of dissociated dislocations to avoid local obstacles by cross-slipping out of their slip plane). The flow stress increases significantly and the dislocation densities attain values where recrystallization can occur during hot plastic deformation.

At low  $Z$  values (typically for Al), plastic flow is purely viscous after an initial transition strain of about 0.1; at a given imposed strain rate the material deforms at constant flow stress. This also corresponds to the creep regime where constant imposed stresses give rise to a continuous shape change, i.e. a roughly constant strain rate. At higher  $Z$  the flow stress also depends on the applied strain, i.e. Note that in typical aluminium hot rolling schedules  $\ln Z$  varies from about 22 in the first passes to about 33 near the end.

In the low  $Z$  regime many studies have shown that the saturation flow stress  $\sigma_s$  can be related to the Zener–Hollomon parameter by a power law:

$$\sigma_s = AZ^m$$

where  $m$  is the strain rate sensitivity, typically 0.1–0.3.

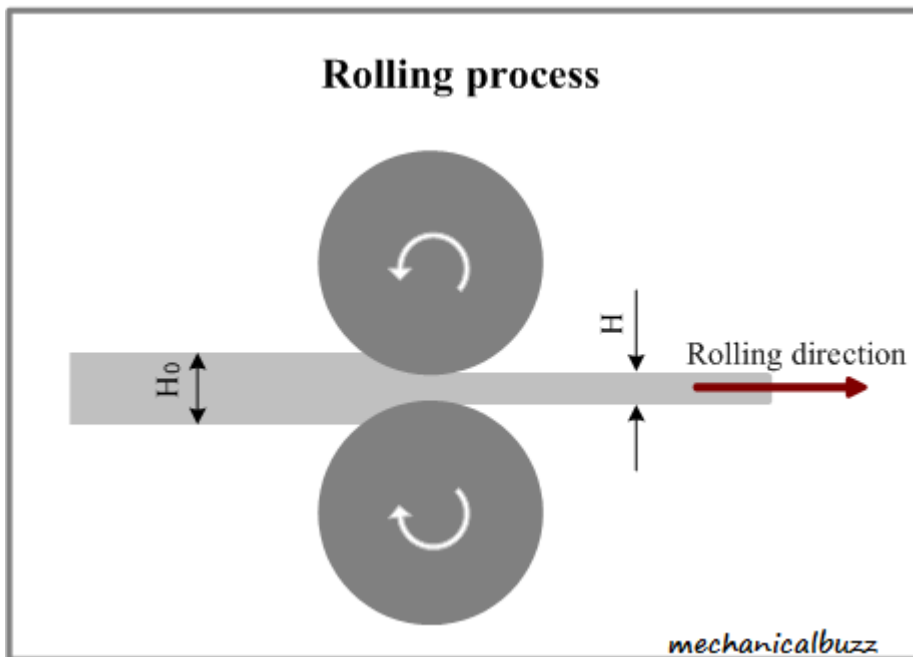
There are various methods of forming steel into finished products, including hot forging, hot and cold rolling, seamless tube making and

welded tube making. The most widely used process is hot rolling, which accounts for over 90% of all steel production.

### 2.3.2 Hot Rolling:

#### Description of Rolling Operation:

Hot rolling involves reheating of ingots, slabs, blooms or billets to the region of 1200 - passed repeatedly back and forth through the same rolls with the roll gap being reduced progressively.



This operation is done in the hot state because the yield strength of steel decreases as temperature rises. Large deformations can thus be obtained with modest roll forces. It is necessary to control both the total reduction, which defines the degree to which the steel is worked, and the reduction in each pass in order to avoid excessive deformation leading to metal cracking or breakage.

The number of passes depends upon the input material and the size of the finished product; it can be as high as 70 before the material becomes too cold to roll down further. Plain barrel rolls are used for flat products such as plate, strip and sheet, while grooved rolls are used for structural sections, rails, rounds, squares, beams, sheet piles, etc.

The basic rolling unit is called a stand and consists of the rolls and a support structure (housing). The rolling mill comprises the stand or group of stands, complete with auxiliary facilities for control and regulation, such as roll drive motors, roller tables for entering and removing the metal, shears, scarfers, etc.

The simplest type of mill consists of a two-high stand. Generally, the two rolls can turn in both directions, which permits reversible operation such that the hot metal is passed repeatedly through the mill in opposite directions achieving progressive reduction in thickness.

When large reductions are required, four-high stands are used to achieve the required high roll forces. The cylindrical work rolls, through which the hot metal passes, are of relatively small diameter and are supported above and below by a second set of larger diameter backing rolls that transmit the force to the work rolls. A four-high stand may also be reversible.

The reduction in thickness of the hot material results in both length increase and sideways spread. The spreading, which depends mainly upon the amount of reduction, temperature, and roll diameter, must be controlled to give the correct dimensions and cross-section. Universal Mills have a set of vertical rolls at the delivery side of the horizontal rolls. In parallel face beam mills, they serve to provide a good dimensional finish to the final product and, in flat product mills, to edge the plates, improving finish and mechanical characteristics.

In addition to its function of shaping the steel into the required size, hot rolling improves the mechanical properties. Correct control of the cast steel chemical composition, final rolling temperature and amount of material reduction is necessary to give products the required physical properties. For certain steel qualities (e.g. high strength with good impact properties at low temperatures) "controlled rolling" or the QST process of quenching and self-tempering of the material during rolling is employed. This process involves either delaying or cooling until a specified lower temperature is reached before the final passes through the mill.

### **HOT ROLLING PROCESSES:**

These processes can be divided into two basic groups

A. Traditional hot rolling-- In traditional hot rolling, the object is to produce the required shape with the minimum number of roll passes

B. Controlled rolling- In controlled rolling, the objective is to increase the strength and toughness of the steel by careful control of temperature and deformation during rolling.

#### **A.Hot rolling**

In traditional hot rolling, temperatures are kept to a maximum so as to reduce the hot strength of the steel and allow large reductions in each roll pass. Because of the high temperature, rapid recrystallization and grain growth occurs between consecutive passes and consequently no grain refinement is achieved. Today, this process is only used for primary reduction and for low-quality steels where there are no specific requirements for strength and resistance against brittle fracture.

## **A. CONTROLLED ROLLING:**

Controlled rolling is a generic term for rolling procedures in which the temperature and deformation during rolling are controlled to achieve desired material properties. Controlled rolling includes:

- Normalizing rolling (N)
- Thermo-mechanical controlled rolling (TMCR). This procedure includes the following processes which employ increased cooling rates, with or without tempering:
  - Accelerated cooling
  - Quenching and Self-Tempering

### **B.1 Normalizing Rolling**

Normalizing rolling is a thermo mechanical treatment during which the final deformation is

Carried out in the normalizing range (950°C). The austenite phase completely recrystallizes between passes but, because of the reduced temperature, does not experience grain growth. Consequently, after the final pass, air cooling produces a material condition equivalent to that obtained after normalizing. The abbreviated designation of this delivery condition is N. Normalizing rolling can be performed on nearly all mills because the final rolling takes place at relatively high temperature such that power and load capacity of the rolling mill is not exceeded.

### **B.2 Thermo-mechanical Controlled Rolling**

Thermo mechanical Controlled Rolling (TMCR) is a thermo mechanical treatment in which the final deformation is carried out in a temperature range where austenite does not recrystallize significantly. On subsequent cooling, the deformed austenite grain structure leads to a final fine grain ferrite-pearlite microstructure. Usually, the final forming takes place at temperatures just above that at which austenite begins to transform into ferrite. Thermo mechanical controlled rolling leads to a material condition which cannot be achieved by heat treatment alone. The resulting grain refined steel shows very desirable toughness properties down to low temperatures for a medium range of product thicknesses and yield strengths. For several years there has been an

increased demand for rolled steel products with yield strengths up to 500 N/mm<sup>2</sup> and in large thicknesses, combined with improved fabrication properties. As TMCR cannot be exploited any further because the mechanical power of the rolling mills is limited, new production technologies have had to be introduced.

### **B.3 Accelerated Cooling**

Accelerated (water) cooling is performed after the final deformation in order to improve mechanical properties by refining the microstructure. This process has a positive influence on strength as well as on toughness properties and allows the alloy content to be lowered compared to TMCR alone. The microstructure of accelerated cooled steels consists mainly of fine-grained ferrite + pearlite and ferrite + bainite, showing low ductile to brittle transition temperatures, i.e. good toughness.

### **B.4 Quenching and Self-tempering**

In the Quenching and Self-Tempering (QST) process, intense water spray cooling is applied to the surface of the product after the last rolling pass, so that the skin is quenched. Cooling is interrupted before the core is affected by quenching and the outer layers are then tempered by the heat flow from the core to the surface during a temperature equalization phase. The QST process has resulted in the creation of a new generation of steel products with high yield strengths up to 500 N/mm<sup>2</sup> and excellent low temperature toughness properties, which are weldable without preheating. Such steels offer important advantages in terms of weight savings and fabrication costs compared to conventionally produced grades.<sup>14</sup>

## **2.3.3 EXTRUSION**

Extrusion is a process in which a billet of metal is first placed into a chamber with a die at one end and a ram on the other. The billet is then pushed through the relatively narrow die to form long profiles of constant section determined by the die geometry.



**Figure 2.3.3** Example of different extrusion profiles.

The process is usually carried out at high temperatures, of the order of  $0.5\text{--}0.75T_m$  to reduce both the applied loads and wear on the dies, but on softer metals can be performed at room temperature. The loads are imposed by mechanical presses or hydraulic rams through a mandrel onto the metal billet, which is restrained by the chamber designed to withstand the large radial stresses generated during extrusion; the above fig is a schematic of the direct extrusion process. According to the die geometry, a very large variety of cross-sections can be produced varying from round or rectangular bars, through L, I or T shapes etc. to tubes and complex sections.

A second type of extrusion – known as ‘indirect or back extrusion’ – uses a hollow ram containing the die, while the other end of the billet is completely blocked off. As the ram is pushed into the billet, the metal is extruded out in the opposite direction through the die (back out along the hollow ram). This has the advantage that there is no relative movement between the container wall and the billet so that the friction forces and the required power level are smaller. However, the use of a hollow ram limits the loads that can be applied.



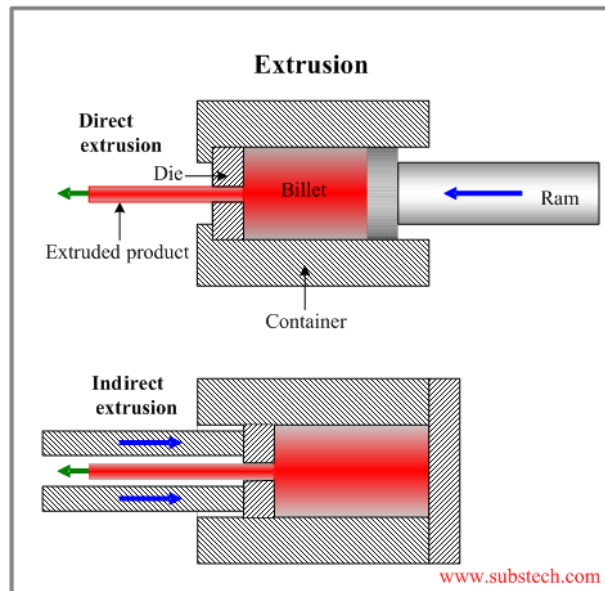


**Figure:2.3.3.**Direct & indirect extrusion processes.

A variant of this is impact extrusion, which is used to produce short lengths of hollow shapes, e.g. toothpaste tubes, from solid rods or disks. A high-speed mechanical press pushes the ram into the disk placed above a female die so that the wall of the can or tube is then punched out between the ram and the die. In general, extrusion tooling is inexpensive; lead times for custom shapes or prototypes are relatively brief and many alloys can be readily formed into complex shapes. Consequently, extrusion has developed significantly over the last two or three decades to become the second most important plastic forming operation, after rolling.<sup>16</sup>

### 2.3.4 WIRE DRAWING

WIRE DRAWING: In a conventional wire drawing process, the diameter of a rod or wire is reduced by pulling it through a conical die (Figure 11.22a). In industrial production lines, a large reduction is obtained by pulling the wire or rod through a series of consecutive dies. In some cases, an intermediate annealing treatment may be necessary.

#### *Wire drawing machines*

Many design variations are available. Single-die machines are relatively simple and are used for breakdown or finishing operations. In most wire drawing plants, several die/capstan combinations are mounted in series to form a continuous wire drawing machine. Since the wire diameter  $D$  is reduced in each pass, the wire speed  $v$  increases after each die. In principle, the following continuity relation must be satisfied:

$$D_{n-1}^2 v_{n-1} = D_n^2 v_n = D_{n+1}^2 v_{n+1}$$

with  $n-1$ ,  $n$  and  $n+1$  successive drawing passes.

### 2.3.5 FORGING:

Forging is the oldest of the metal forming processes. **Forging** is a manufacturing process involving the shaping of metal using localized compressive forces. Forging is often classified according to the temperature at which it is performed: "cold", "warm", or "hot" forging.

In modern times, industrial forging is done either with presses or with hammers powered by compressed air, electricity, hydraulics or steam. These hammers may have reciprocating weights in the thousands of pounds.

## **PROCESSES:**

All of the following forging processes can be performed at various temperatures, however they are generally classified by whether the metal temperature is above or below the recrystallization temperature. If the temperature is above the material's recrystallization temperature it is deemed *hot forging*; if the temperature is below the material's recrystallization temperature but above 30% of the recrystallization temperature (on an absolute scale) it is deemed *warm forging*; if below 30% of the recrystallization temperature (usually room temperature) then it is deemed *cold forging*. The main advantage of hot forging is that as the metal is deformed work hardening effects are negated by the recrystallization process. Cold forging typically results in work hardening of the piece.

## **DROP DRAWING:**

Drop forging is a forging process where a hammer is raised and then "dropped" onto the work piece to deform it according to the shape of the die. There are two types of drop forging: *open-die drop forging* and *closed-die drop forging*.

### ***Open-Die Drop Forging:***

In open-die forging, a hammer strikes and deforms the work piece, which is placed on a stationary anvil. Open-die forging gets its name from the fact that the dies (the surfaces that are in contact with the work piece) do not enclose the work piece, allowing it to flow except where contacted by the dies. Therefore the operator, or a robot, needs to orient and position the work piece to get the desired shape. Open-die forging lends itself to short runs and is appropriate for art smiting and custom work.

#### **Advantages of Open-Die Forging**

- Reduced chance of voids
- Better fatigue resistance
- Improved microstructure

- Continuous grain flow
- Finer grain size
- Greater strength

### **Closed-Die Drop Forging:**

In closed-die forging, the metal is placed in a die resembling a mould, which is attached to the anvil. Usually, the hammer die is shaped as well. The hammer is then dropped on the work piece, causing the metal to flow and fill the die cavities. The hammer is generally in contact with the work piece on the scale of milliseconds. Depending on the size and complexity of the part, the hammer may be dropped multiple times in quick succession. Excess metal is squeezed out of the die cavities, forming what is referred to as *flash*. The flash cools more rapidly than the rest of the material; this cool metal is stronger than the metal in the die, so it helps prevent more flash from forming. This also forces the metal to completely fill the die cavity.<sup>2</sup>

# CHAPTER 3

## EXPERIMENTAL PROCEDURE

## **EXPERIMENTAL PROCEDURE**

---

### **3.1 METALLOGRAPHY**

#### **3.1.1 Sample Preparation:**

The preparation of the metallographic specimens generally involves five major operations:

- a) Sectioning of the samples
- b) Mounting of the samples  
(optional)
- c) Grinding of the samples
- d) Polishing of the samples and
- e) Etching of the samples.

#### **a)SECTIONING:**

The sectioning of the samples is done by firstly setting the sample in a bench vice. The sample is then cut by using a hack saw into a minimum uniform cross sectional area, using which the metallographic operation can further be performed on the given sample.

### **b) MOUNTING:**

The samples are then mounted by the normal cold mounting process prior to the experiments. The cold mounting material used was epoxy resin.



Fig.3.1.1.a Mounting of sample

### **c) BELT POLISHING**

The rough grinding operation was performed on the samples using a belt grinder. This was done in order to remove any unnecessary excessive material (chips) from the surface of the sample. The secondary grinding of the samples was done further by using Emery paper. The emery papers used were of nos. 120, 180, 1/0, 2/0 respectively.



Fig:3.1.1.b Polishing Belt

#### d) **POLISHING OF SAMPLE**

The term polishing is mainly aimed at explaining the various final polishing process that are involved in the further metallography testing of the samples. These various processes of final polishing involves the use of cloth-covered laps and suitable polishing abrasives. The cloth-covered laps have either a rotating or a vibrating motion. The specimen to be polished is held by hand within the polishing area. Aluminium oxide (Alumina) was used as an abrasive. This operation is performed in order to provide its surface a mirror finish.



Fig.3.1.1.c Polishing of specimen in polishing wheel

#### e) **ETCHING:**

After the cloth polishing of the sample is etched. A solution containing 2% conc. nitric acid ( $\text{HNO}_3$ ) and 98% ethyl alcohol, called 2% Nital, is used as an etchant. Etching of the sample is performed in order to have a better resolution of the microstructure using microscopes.





Fig:3.1.1.d Etching.

### 3.1.2 OPTICAL MICROSCOPY

The microscope that is used for the specimen illustration or obtaining the microstructure of the given samples is a Metallurgical microscope. The metallurgical microscope is type of optical microscope only, but differ from the other microscopes in the method by which the specimen illustration is done. Frontal lighting is used in the metallurgical microscopes for illuminating the metal surface. The frontal lighting illumination is done because metals are opaque substances. This is achieved by using a plain glass reflector that is installed in the tube. A schematic diagram of the optical microscope is shown below in Fig. 3.1.2

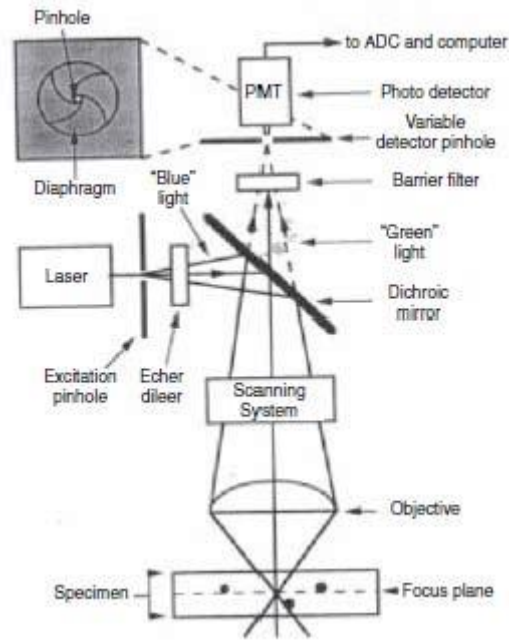


Fig. 3.1.2: Schematic diagram of the optical microscope.



Fig. 3.1.2The Optical microscope used while performing the tests.

### 3.1.3 SCANNING ELECTRON MICROSCOPY (SEM)

Scanning electron microscope (Fig. 3.3) uses focused beam of electrons, scanning in vacuum the specimen surface, imaging one point at a time. The interaction of the electron beam with every point of the specimen surface is registered, forming the entire image. Since the wavelength of the electron beam is much lower than the wavelength of the visible light, the magnification of SEM is much higher, nearly thousands of times, than that of the optical microscopes. Resolution of SEM is about 1nm to 20nm.

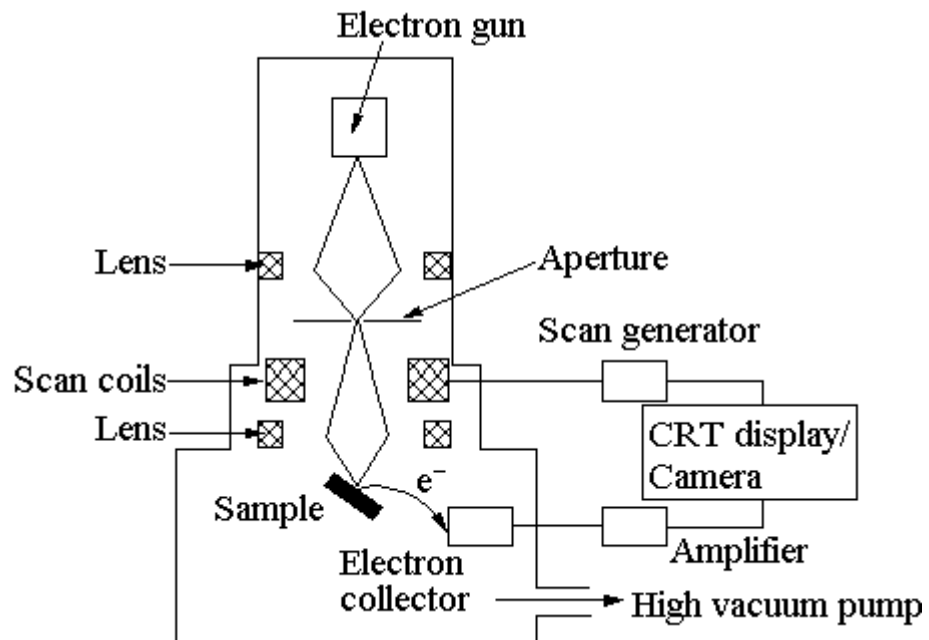


Fig: 3.1.3 Scanning Electron Microscope



Fig 3.1.3 SEM used while performing the tests.

### 3.1.4 VICKERS MACRO HARDNESS TEST

The Vickers hardness test is performed using a 136 degree square base pyramidal diamond indenter that forms a diamond indent on the surface of the material to be tested. The indenter is pressed into the sample by using an accurately controlled test force. The force is maintained for a specific dwell time of 10 to 15 seconds. After the dwell time is complete, the indenter is removed leaving an indent in the sample that appears as square shaped on the surface. The size of the indent is measured optically by measuring the two diagonals of the indent using the microscope provided. The Vickers hardness number is calculated as a function of the test force divided by the surface area of the indent. The average of the two diagonals is used in the following formula to calculate the Vickers hardness:

$$HV = (\text{Constant} * \text{Test force}) / \text{indent diagonal squared}$$

$$HV = 2P \sin(\theta/2) / d^2 = 1.854P / d^2$$

Where  $P$  = Applied Load (in kg)

$d$  = Average length of the diagonals (in mm)

$\theta = 136$  degree

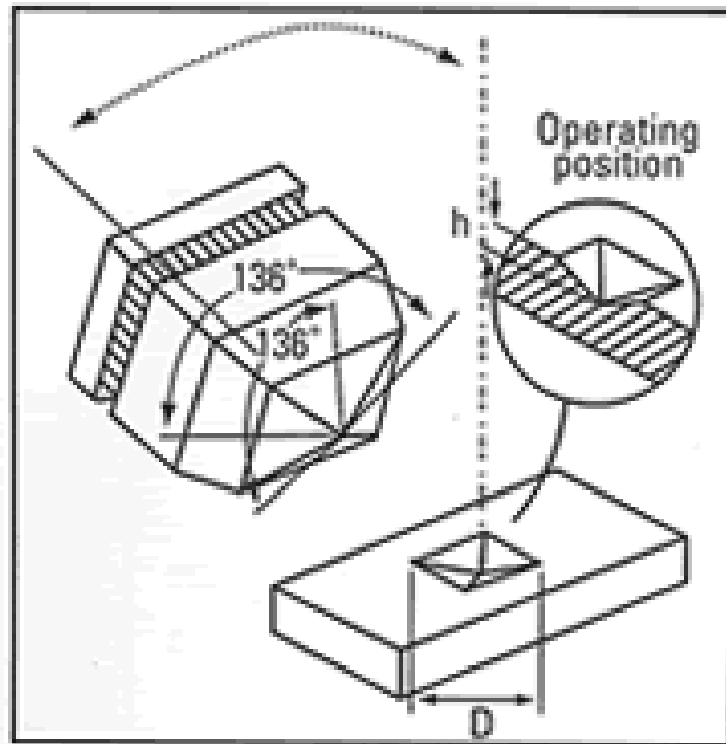


Fig 3.1.4: Vickers Indenter



Fig 3.1.4 Macro-hardness tester used -VM 50

### 3.1.5 X-ray Powder Diffraction (XRD):

#### Theory:

From the year 1912, the application of x-ray has started when the wave nature of x-ray was established from the x-ray diffraction by any crystals. X-ray diffraction by the different set of planes has been applied to identify crystal structures. The basic law involved in the diffraction method of structural analysis is the Bragg's law. When monochromatic x-rays impinge upon the atoms in a crystal lattice, each atom acts as a source of scattering. The crystal lattice acts as series of parallel reflecting planes. The intensity of the reflected beam at certain angles will be maximum when the path difference between two reflected waves from two different planes is an integral multiple of  $\lambda$ . The law that governs all diffraction phenomena in x-ray diffraction is the "Bragg's Law"

$$2d\sin\theta = n\lambda$$

Where  $d$  is the inter planer spacing,  $\theta$  and  $\lambda$  are the incident angle and wavelength of x-ray respectively. The schematic diagram of x-ray diffraction is shown in Fig.3.1.5.a .

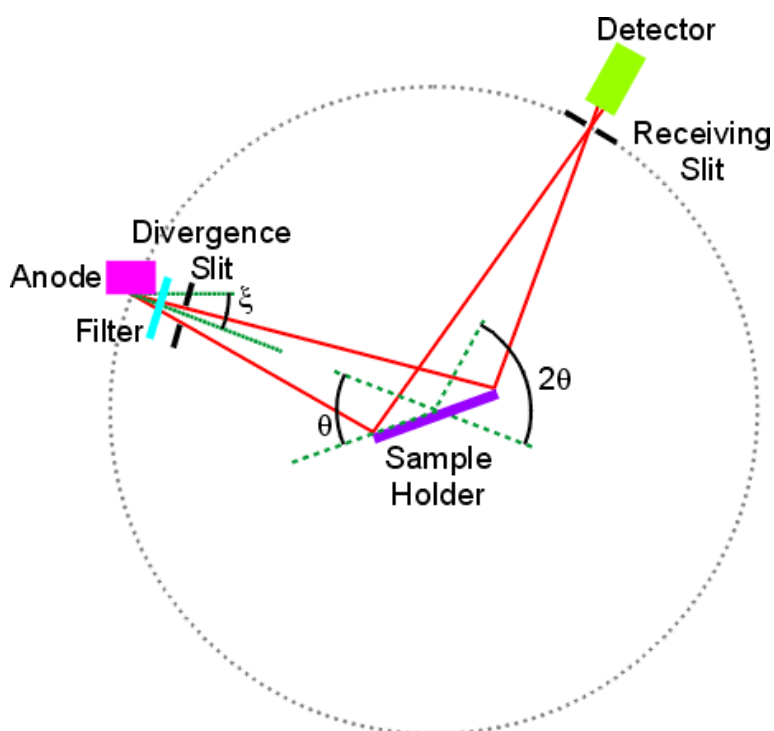


**Fig.3.1.5.a: Schematic diagram of x-ray**

The x-rays used in diffraction have wavelength lying approximately in the range of 0.5-2.5 Å. Sets of atomic planes within the crystal will cause constructive interference if the incident beam hits them at the Bragg angle. Atomic planes, from which the  $d_{hkl}$  values are determined, are indexed using conventional Miller Index notation. In a crystal structure there may be several groups of parallel lattice planes. Each set of planes will produce an interference peak from x-ray diffraction. The overall diffraction pattern will thus contain several diffraction peaks. Since it's the  $d$  value that is to be

calculated, from the Bragg equation either  $\theta$  or  $\lambda$  is varied and the other is measured. Based on this there are three methods of structural analysis viz., Laue technique, rotating crystal method and powder technique. The variables in these methods are:<sup>17</sup>

**Different method of XRD measurements:**

Method	Wave-length ( $\lambda$ )	Incident angle ( $\theta$ )
Laue Method	Variable	Fixed
Rotating-crystal Method	Fixed	Variable
Powder Method	Fixed	Variable

**Particle size determination by Scherrer formula:**

Experimentally obtained diffraction patterns of the sample are compared with the standard powder diffraction files published by the JCPDS. The average grain size of the samples was

calculated using the **Scherrer's formula**,

$$D = 0.9\lambda / \beta \cos\theta$$



Where  $\lambda$  is the wavelength of the x-rays and  $\beta$  is the full width at half maximum intensity in radians.

It is important to realize that the Scherrer formula provides a lower bound on the particle size. The reason for this is that a variety of factors can contribute to the width of a diffraction peak; besides particle size, the most important of these are usually is dependent on the factors like inhomogeneous strain and instrumental effects. If all of these other contributions to the peak width were zero, then the peak width would be determined solely by the particle size and the Scherrer formula would apply. If the other contributions to the width are non-zero, then the particle size can be larger than that predicted by the Scherrer formula, with the "extra" peak width coming from the other factors.

A Rigaku Ultima III X-ray diffractometer was used for recording the diffraction traces of the samples in  $\theta$ - $2\theta$  mode with monochromatized Cu  $K\alpha$  radiation, ( $\lambda = 1.5404\text{\AA}$ ) operated at 40 KV voltage and 30 mA current. A photo graph of X-ray diffractometer is shown in figure 3.1.5.b .



**Fig.3.1.5.b: Rigaku Ultima III X ray diffractometer**

# **CHAPTER 4**

## **RESULTS & DISCUSSION**

## RESULT AND DISCUSSION

---

### 4.1. Kick Rod of a Bike:

The specimen of Kick Rod steel is shown in Fig 4.1.1. The details of dimensions are given below:

Sample name : Kick Rod of a Bike.

Kick Rod dia. 14.4 mm



Fig 4.1.1 Kick Rod steel

#### 4.1.1 Source

The sample was collected from a bike part shop.

#### 4.1.2 Chemical Composition:

The chemical composition of the low carbon steel sample (Table-4.1.2) was determined by XRF. The specimen carbon is 0.189% which is low carbon.

Elements	Value	Elements	Value	Elements	Value	Elements	Value
C %	0.189	Cu %	0.0277	Bi %	0.00868	Mo %	0.00515
Si %	0.151	Al %	0.00590	Ca %	0.00039	B %	0.00082
Mn %	0.489	Sn %	0.00256	Ce %		Nb %	0.00446
P %	0.0163	Ti %	0.00082	Co %	0.00246	Pb %	0.0104
S %	0.0128	V %	0.00314	Fe %	98.9	Sb %	<0.0025
Cr %	0.0654	W %	0.0151	La %	0.00312	Ta %	<0.0100
Ni %	0.0180	As %	0.00237	N %	<0.0022	Zr %	0.00096

Table : 4.1.2 chemical composition of kick rod

### 4.1.3 Optical Microscopy

The microstructures of Kick Rod steel are shown in Fig.4.1.3.a, Fig.4.1.3.b and Fig.4.1.3.c . The structure consists of bcc, with fine pearlite elongated along cold rolling direction .It also exhibits few pearlite colonies as usual low carbon steel .

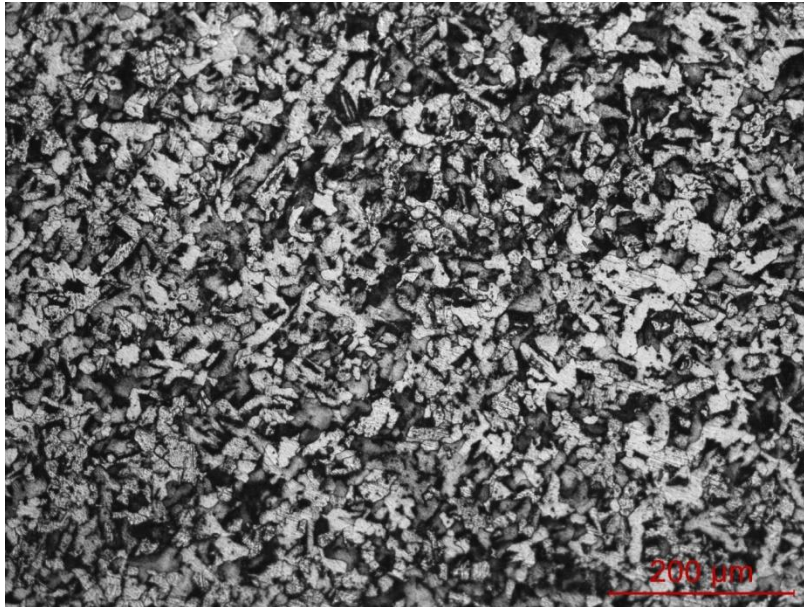


Fig. 4.1.3.a:[100X Etchant-2% nital ]. The microstructure consists of the ferrite & pearlite .

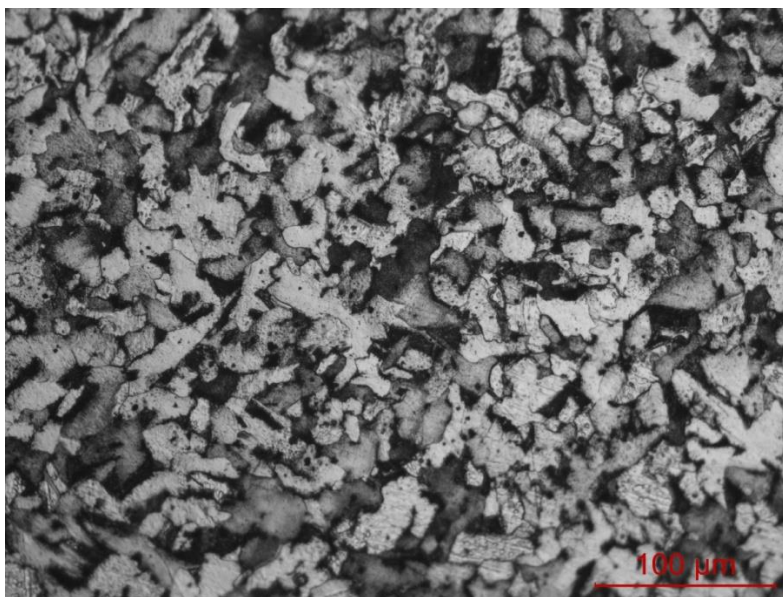


Fig. 4.1.3.b:[200X Etchant-2% nital ]. The microstructure consists of the ferrite with pearlite with irregular shaped grains.

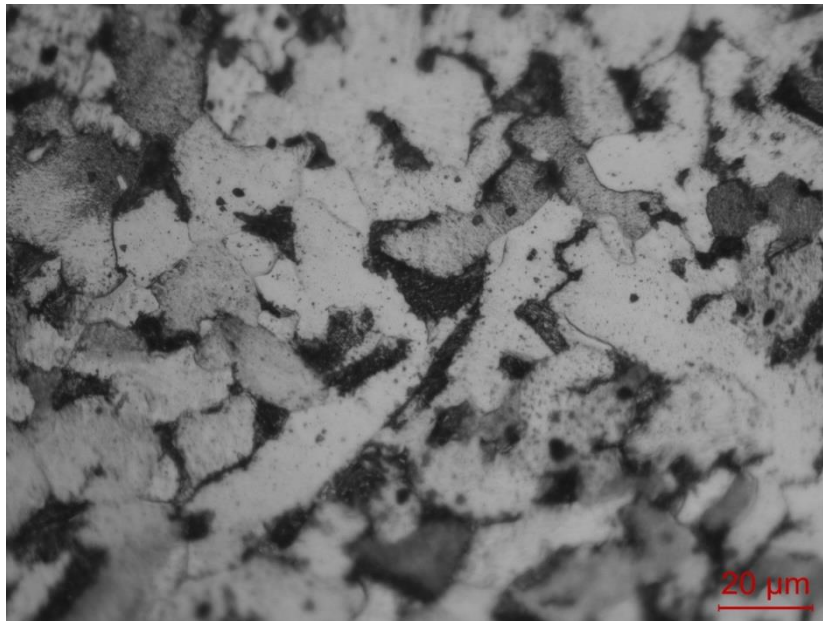


Fig. 4.1.3.c:[500X Etchant-2% nital ]. Some inclusions are identified in the grains

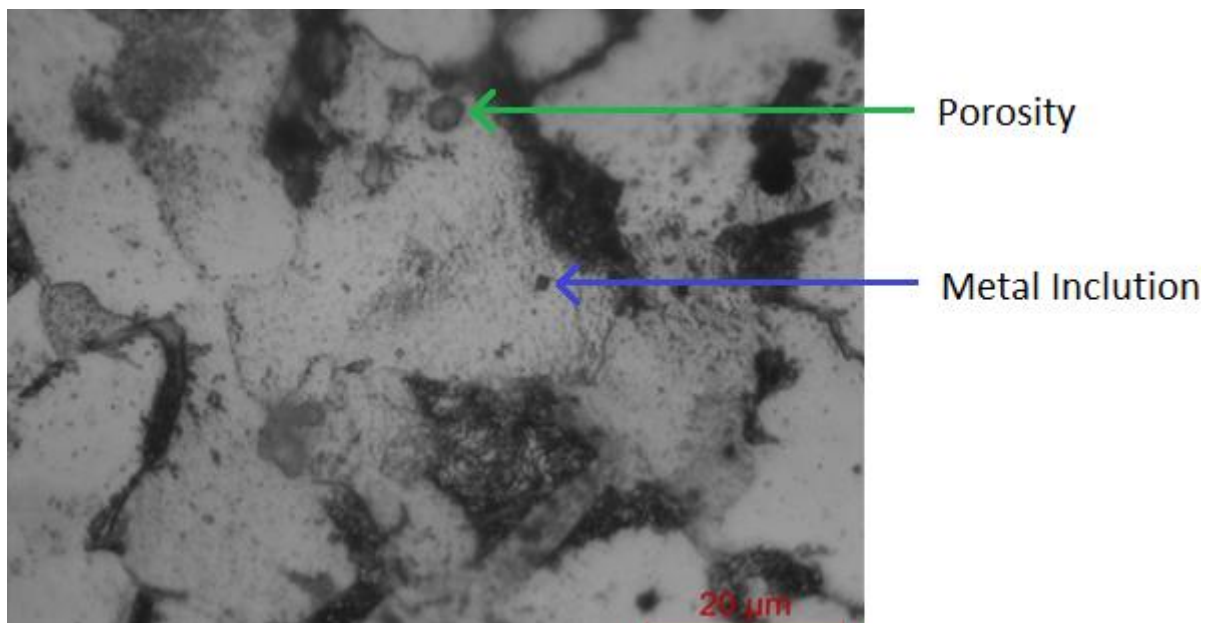


Fig. 4.1.3.d:[1000X Etchant-2% nital ]. The microstructure consists of ferrite with pearlite with some pores and inclusions.

Observations: The above studies indicate large amount of ferrite formation and pearlite are scattered between grains of ferrite. Large amount of inclusions have been noticed with pores in the grains at higher magnifications of micrographs.

#### 4.1.4 SEM RESULTS:

The SEM images of Kick Rod steel have been presented in the Fig4.1.4 and Fig4.1.5. The microstructure confirms ferrite & pearlite structure

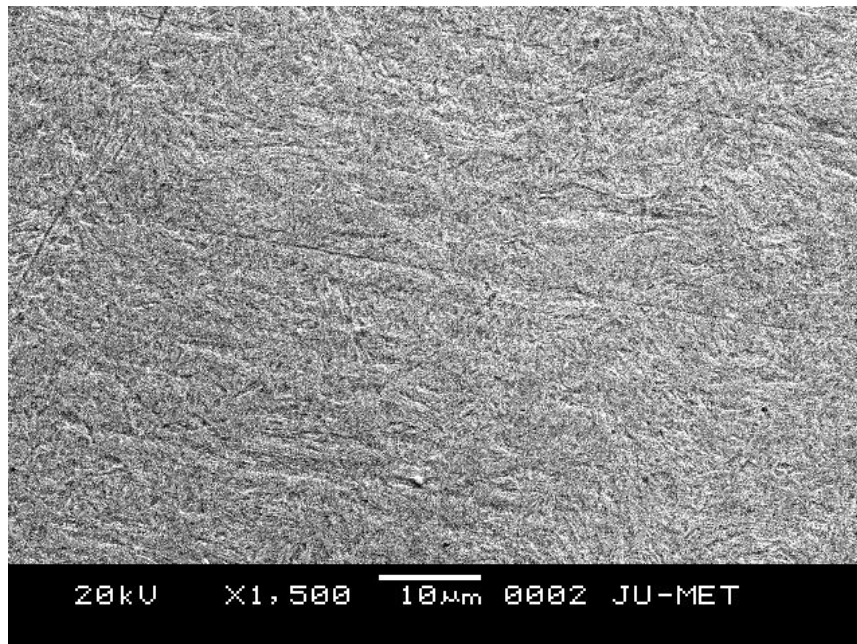


Fig. 4.1.4: [1500 X Etchant-2% nital].

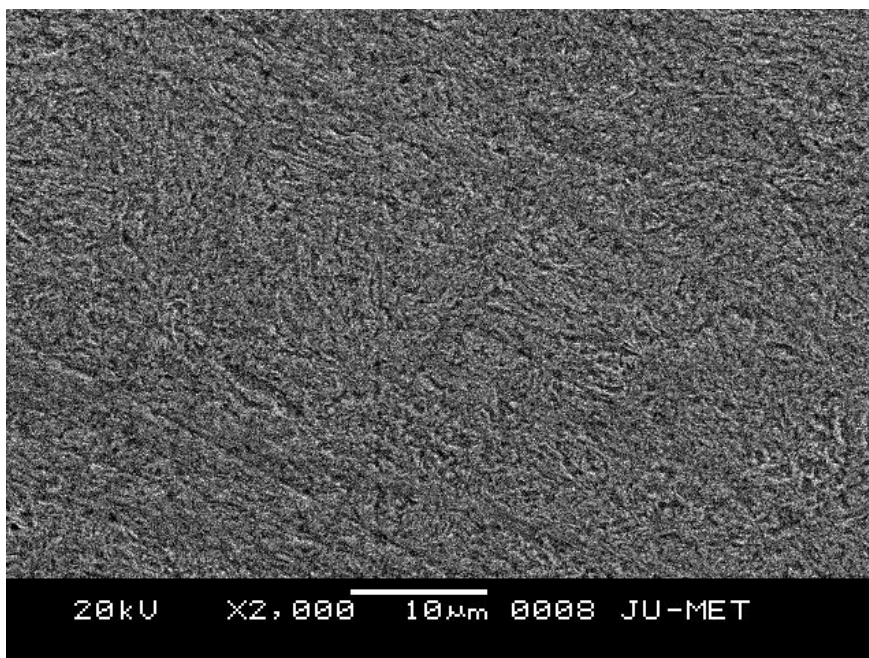


Fig. 4.1.4: [2000 X Etchant-2% nital].



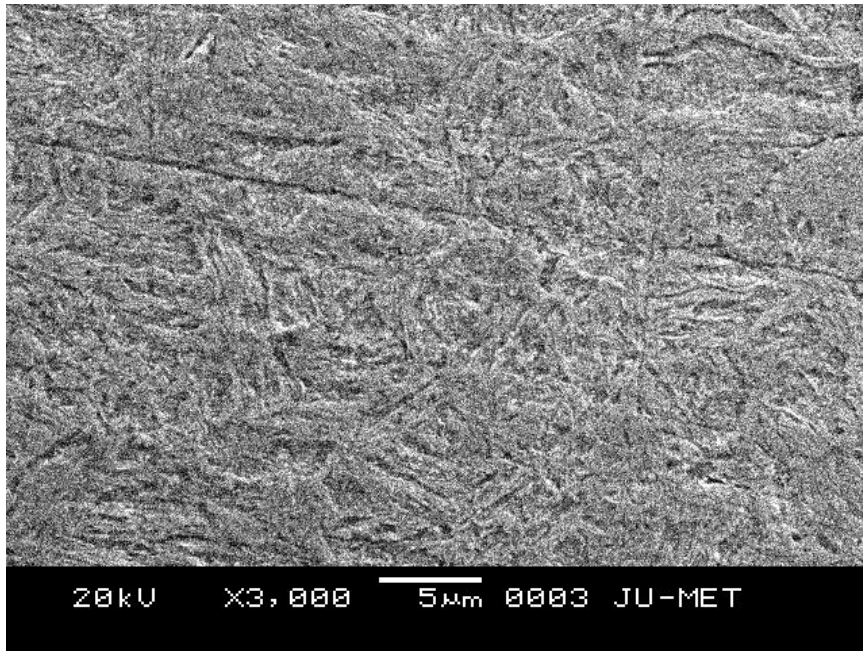


Fig. 4.1.4: [3000 X Etchant-2% nital. In higher magnification ferrite & pearlite are also more Prominent with elongated structure due to rolling.

Observations: All the SEM micrograph indicate presence elongated ferrite & pearlite with lamellar band structure. The product seems to be rolled and platelets fibrous structure is formed. Some voids are noticed.

#### 4.1.5 Phase analysis by XRD

The X-Ray diffraction pattern on the Kick Rod steel of a bike has been given in the Fig 4.1.5 and Table 4.1.5. Comparing with the JCPDS file  $\alpha$ -ferrite phase is confirmed . Pearlite and ferrites both are present in the structure

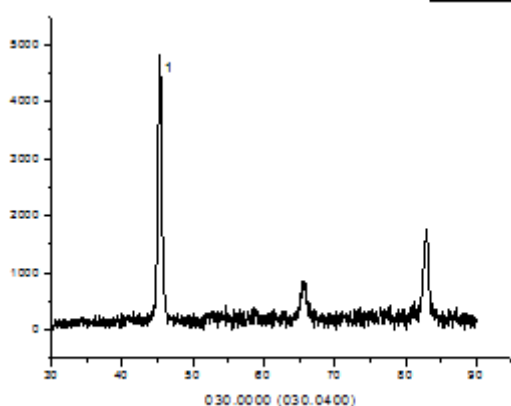


Fig:4.1.5 XRD spectra of kick rod

Peak No.	2 theta	FWHM	d-value	intensity	I/I0	Identified Phase
1	45.0280	0.659	2.0010	1401	100	$\alpha$ -ferrite, Cementite
2	65.680	1.082	1.42	175	13	$\alpha$ -ferrite
3	82.940	0.800	1.16	413	30	$\alpha$ -ferrite

Table :4.1.5 XRD spectra of kick rod

#### 4.1.6 Vickers Hardness Test Results:

Vickers Hardness test results on the sample (Kick Rod steel) are given in the Table 4.1.6. The load is given 30 Kg. The average hardness of steel material has been found to be 146.26HV. The low hardness testifies application of softening to achieve deep drawing property of forming.

Serial no.	Length of one diagonal (d1)mm	Length of other diagonal (d1)mm	Average	Hardness (VHN) Kgf/mm <sup>2</sup>
1	.641	.642	.642	156.26

Table :4.1.6 Vickers Hardness Test of kick rod

#### 4.1.7 Tensile Test Results:

Tensile test was carried out as per ASTM E-8 standard at room temperature. The test was also carried out in a computerised (INSTRON-8801) electro mechanical testing machine and load versus displacement was recorded. Four identical test samples were tested and the average value of these samples was taken as the respective test data.



FIG:4.1.7.a Tensile hardness machine(INSTRON-8801)

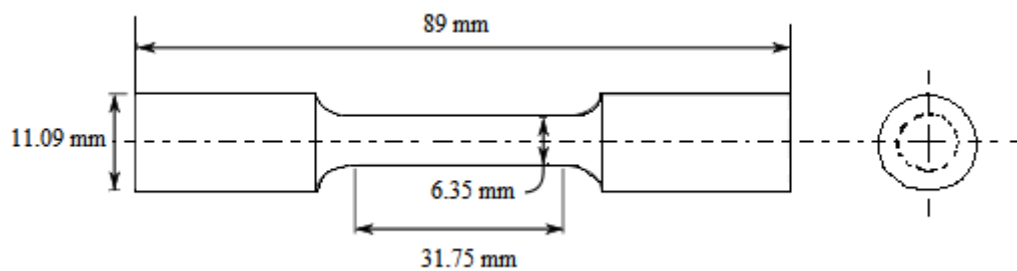
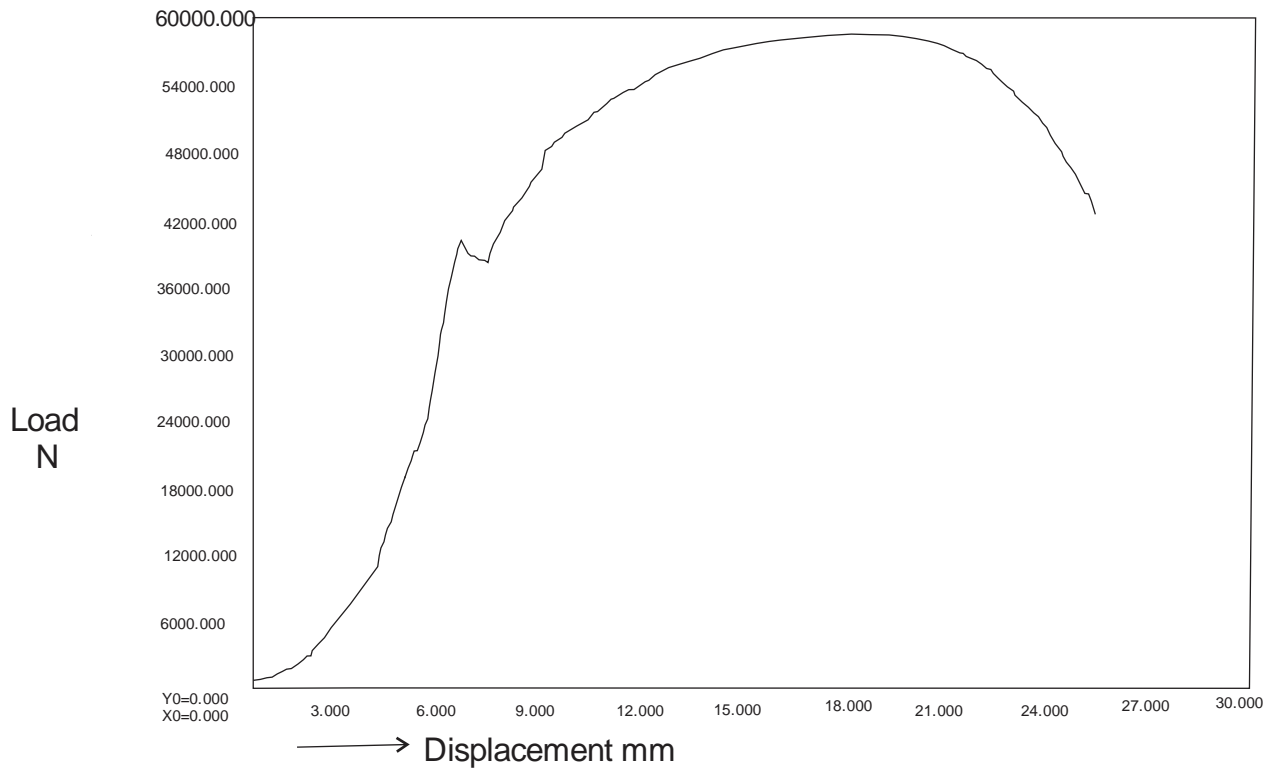


FIG:4.1.7.b Tensile sample preparation

	Yield stress, $\text{N/mm}^2$	Ultimate Tensile Strength, $\text{N/mm}^2$	% Elongation on 50 mm G.L
<b>FINDING</b>	326 (three hundred twenty-six)	471 (four hundred seventy-one)	31 (thirty-one)

Table : 4.1.7 Tensile Hardness Test of kick rod

Graph: Load Vs Displacement



Graph:4.1.7 Load vs Displacement

Result of : Tensile Test of kick rod

Maximum Force : 58 N

## 4.2 Lever Arm of a bike:

The specimen of steel used in liver arm of bike is shown in the Fig 4.2 :



Fig:4.2 Lever Arm of a bike

### 4.2.1 Source:

The sample was collected from a bike workshop.

### 4.2.3 Chemical Composition:

The chemical composition of the steel used in the lever arm has been tabulated in the Table 4.2.3. The chemical composition is indicative of Ni-Cr-Mo steel. The carbon equivalent of this sample was found to be 0.258% .

Elements	Value	Elements	Value	Elements	Value	Elements	Value
C %	0.258	Cu %	0.145	Bi %	<0.0001	Mo %	0.033
Si %	0.165	Al %	0.17	Ca %	<0.0029	B %	0.00088
Mn %	0.429	Sn %	0.0017	Ce %	<0.0003	Nb %	0.0017
P %	0.018	Ti %		Co %	0.026	Pb %	
S %	0.033	V %	0.011	Fe %	98.28	Sb %	0.0046
Cr %	0.144	W %	0.025	La %		Ta %	
Ni %	0.363	As %	<0.0010	N %		Zr %	

Table:4.2.3 Chemical Composition of the lever arms

#### 4.2.4 OPTICAL MICROSCOPE

The microstructure of the sample has been given in the figure 4.2.4.a and fig:4.2.4.b .It shows the ferrite and pearlite almost in equal proportion.

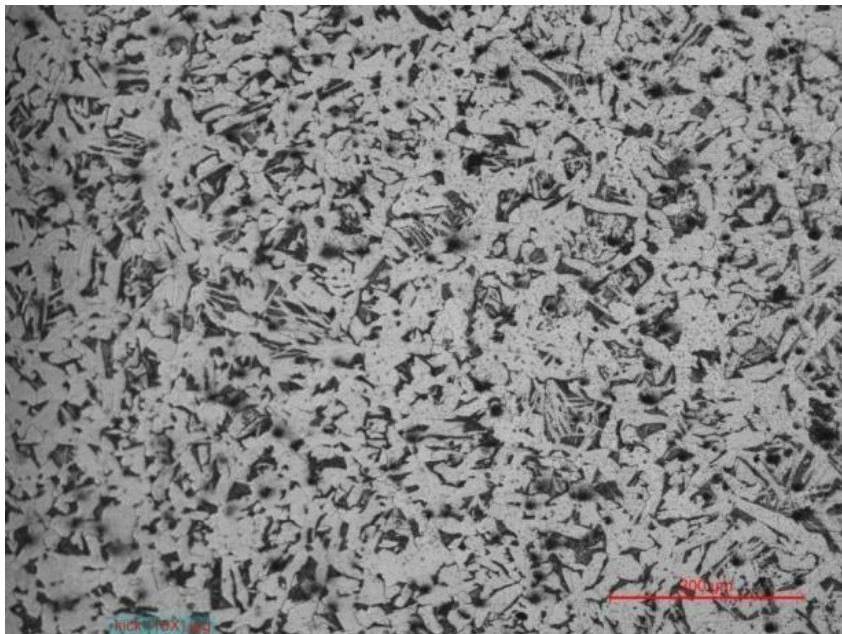


Fig. 4.2.4.a:[50 X Etchant-2% nital ] Ferrite and pearlite microstructure has been revealed where distortion of the phases due to forging has been found.

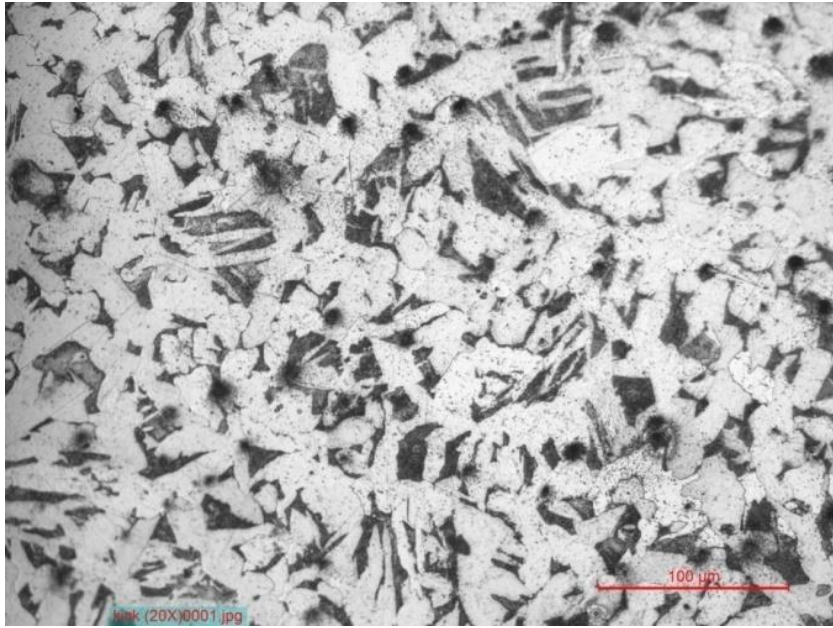


Fig. 4.2.4.b:[100X Etchant-2% nital ] Ferrite and pearlite microstructure has been revealed in the figure.The pearlite phase is very clear in the micrograph.

#### 4.2.5 SEM analysis :

The SEM images of sample have been presented in the Fig4.2.5. The microstructure shows high resolution of fine pearlite . Few grains of  $\alpha$ -ferrite have also been suggested in the structure which reinforces the strength of the steel as well as its toughness.

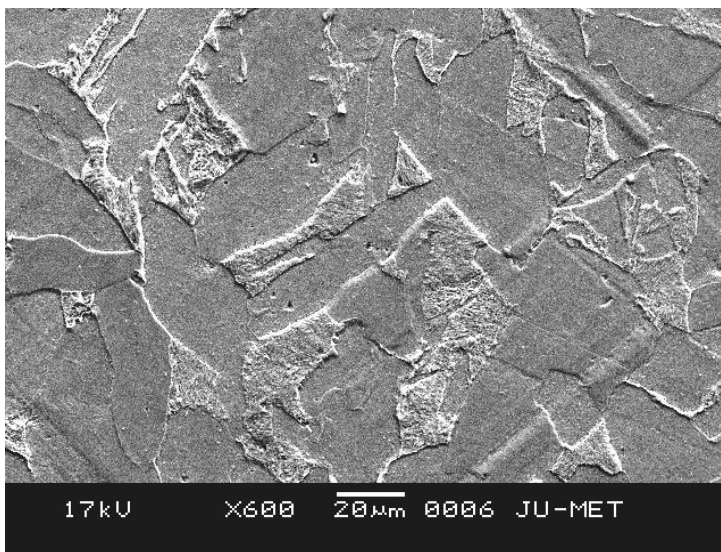


Fig. 4.2.5:[600 X Etchant-2% nital ] The microstructure shows high resolution of fine pearlite.

#### 4.2.6 Phase analysis of XRD:

The X-Ray diffraction pattern on steel used in liver arm of bike has been given in the Fig 4.2.6 and Table 4.2.6. Comparing with the JCPDS file ferrite phase and carbide phase are confirmed .

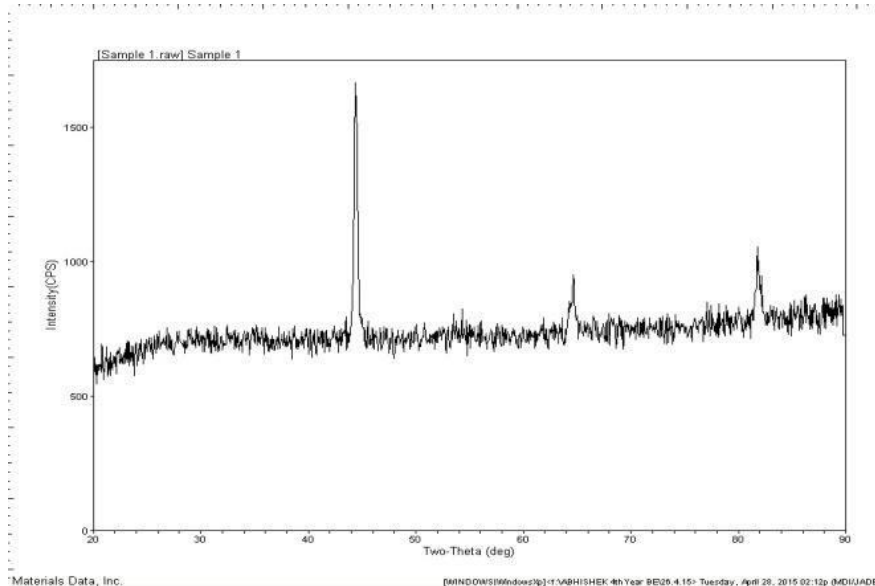


Fig. 4.2.6 XRD spectra of the lever arm

Peak No.	2 theta	d-value	intensity	I/I0	Identified Phase
1	44.4	2.0003	1401	100/210	$\alpha$ - ferrite,Cenetite
2	64.63	1.44	175	13	$\alpha$ - ferrite
3	81.75	1.19	413	30	$\alpha$ - ferrite

Table 4.2.6 XRD spectra of the lever arm

#### 4.2.7 Vickers Hardness Test

##### Results:

Vickers Hardness test (Macro) results on the sample (steel used in liver arm of bike) are given in the table 4.2.7 . The hardness of steel material has been found to be 134.95 HV



Serial No.	Load (in kgf)	Length of One Diagonal (d1 mm)	Length of the other diagonal (d2 mm)	Average (d mm)	Hardness (VHN) kgf/mm <sup>2</sup>
1	30	0.642	0.642	0.642	178.3

Table:4.2.7 Vickers Hardness Test of lever arm

### 4.3. chain of a bike

The specimen of chain of a bike is shown in Fig 4.3. .



Fig: 4.3. chain of a bike

#### 4.3.1 Source

This bike chain was collected from a bike repairing workshop.

### 4.3.2 Chemical Composition:

The chemical composition of Bike chain is given in Table 4.3.2. The amount of C (.370 %) in the steel suggests it is medium carbon steel .

Elements	Value	Elements	Value	Elements	Value	Elements	Value
C %	0.370	Cu %	0.0697	Bi %	0.0363	Mo %	0.190
Si %	0.240	Al %	0.0181	Ca %	~0.0060	B %	<0.0001
Mn %	0.611	Sn %	0.00102	Ce %		Nb %	0.00738
P %	0.0160	Ti %	0.00303	Co %	0.00453	Pb %	0.00521
S %	0.0143	V %	0.00531	Fe %	97.2	Sb %	<0.0025
Cr %	0.0600	W %	<0.0050	La %	0.00818	Ta %	<0.0100
Ni %	0.0162	As %	<0.0005	N %	>0.0396	Zr %	0.00465

Table: 4.3.2 Chemical Composition

### 4.3.3 Optical Microscopy

The microstructure of Bike chain is given in Fig 4.3.3.a and 4.3.3.b . The microstructure indicates ferrite grains and presence of some inclusions.

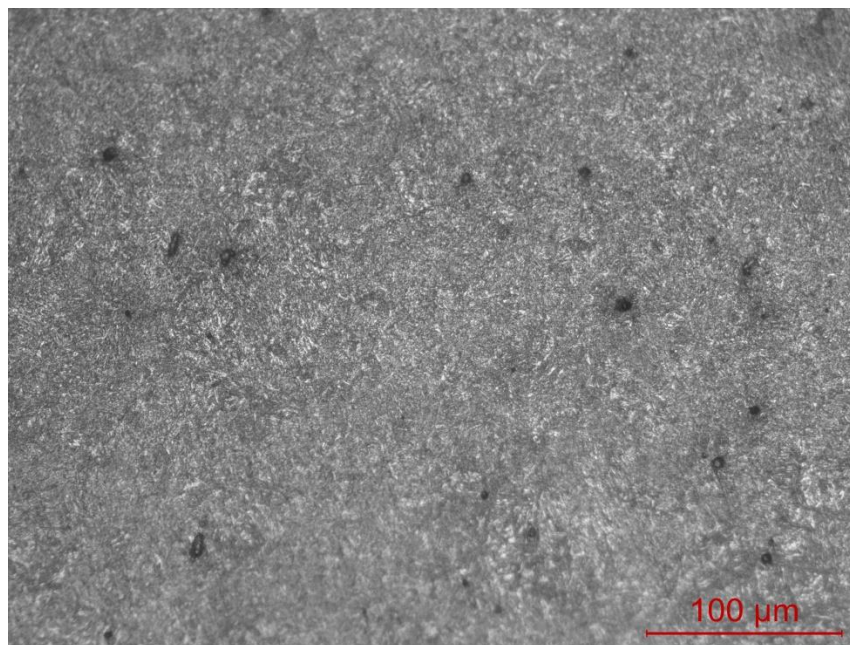


Fig. 4.3.3.a: [50X Etchant-2% nital ] The rolling direction can be easily viewed in the above image.



Fig. 4.3.3.b: [100 X Etchant-2% nital ] The microstructure taken at cross section shows pancake structure of ferritic and pearlitic grains.

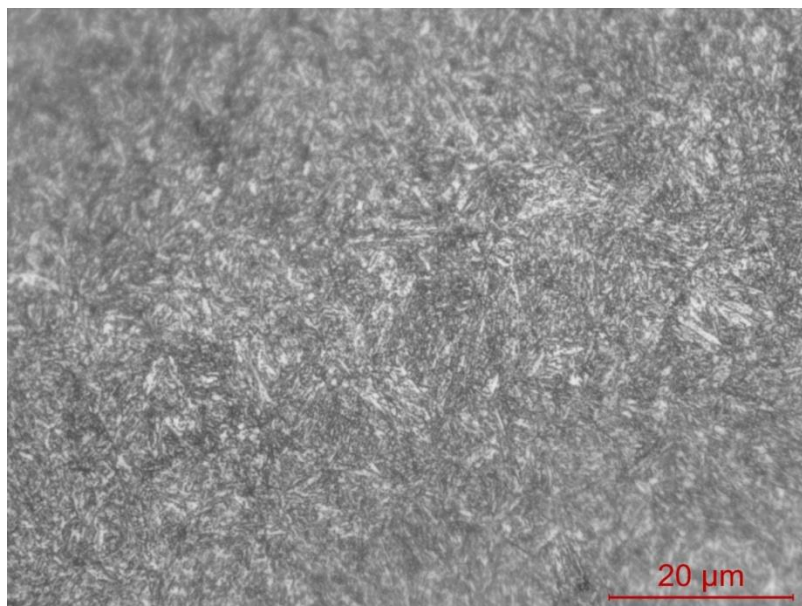


Fig. 4.3.3.c: [200 X Etchant-2% nital ] The microstructure taken at cross section shows pancake structure of ferritic & pearlitic grains.

#### 4.3.4 SEM ANALYSIS:

The SEM images of Bike have been presented in the Fig 4.3.4.a and Fig 4.3.4.b . The microstructure reveals equi-axed ferrite & pearlite grains with inclusions.

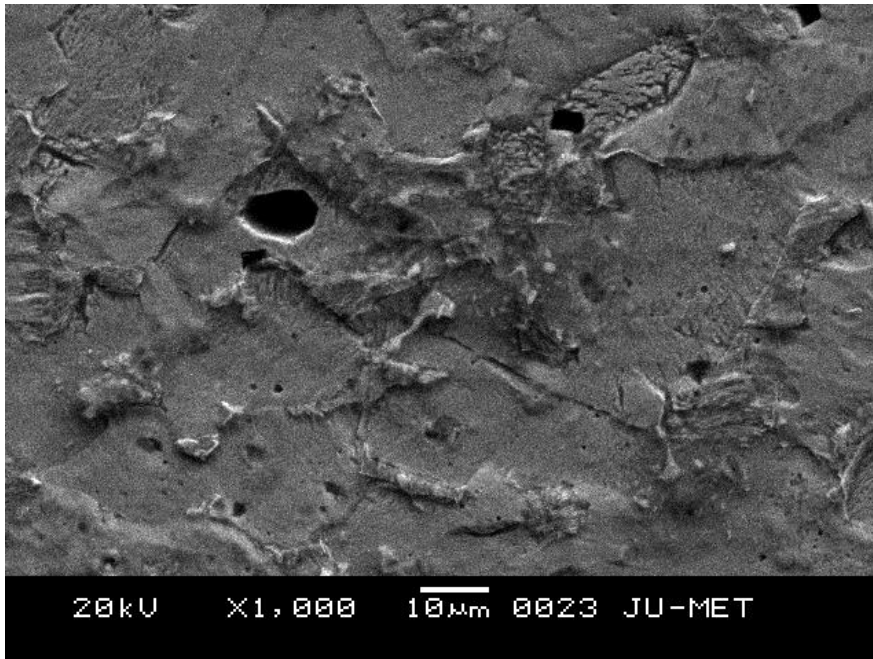


Fig. 4.3.4.a: [1000 X Etchant-2% nital ] The image shows prominent grain boundaries of ferritic grains with some abnormally large grains

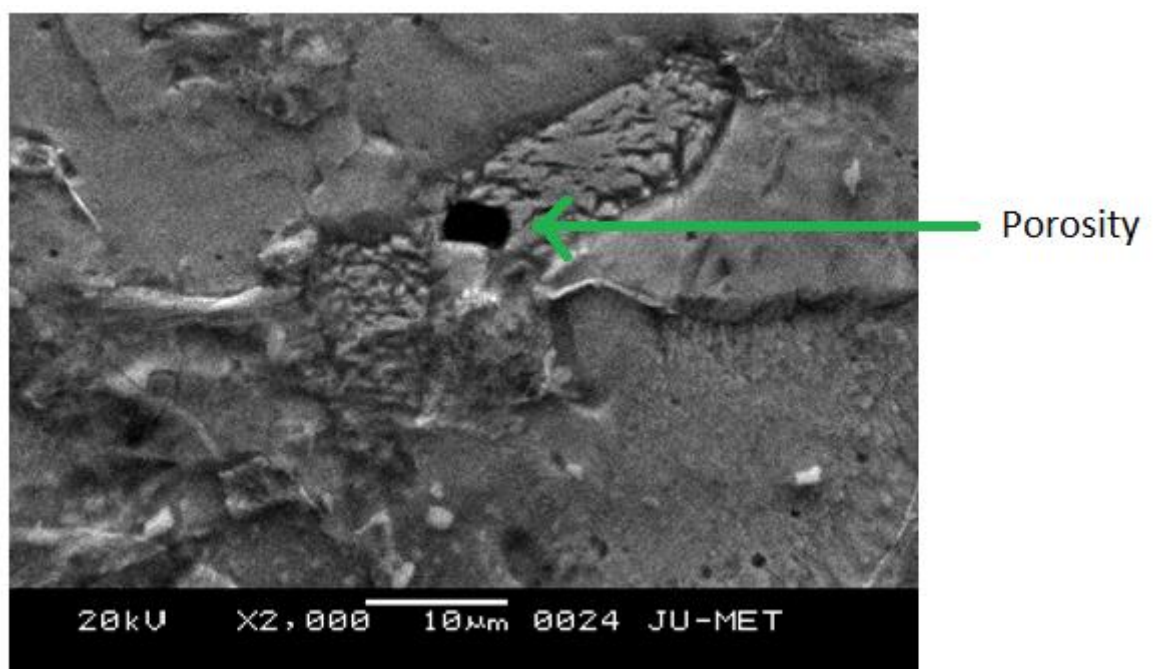


Fig. 4.3.4.b: [2000 X Etchant-2% nital ]. At higher magnification the equiaxing nature of grains is clearly highlighted.

#### 4.3.5 Phase Analysis by XRD :

The X-Ray diffraction pattern on Bike chain has been given in the Fig 4.3.5 and Table 4.3.5. Comparing with the JCPDS file  $\alpha$ -ferrite phase is confirmed also cementite phase

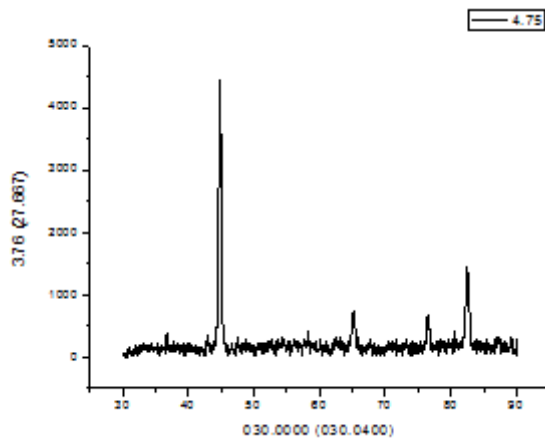


Fig:4.3.5 XRD Spectra of bike chain

Peak No.	2θ	d(A)	Intensity	Relative Intensity(I/I <sub>0</sub> )	Identified Phase	Diffracting Plane(hkl)
1	44.80	2.0213	1798	100	αFerrite/cementite	110
2	65.080	1.4320	249	14	Ferrite	110
3	82.400	1.1694	613	36	αFerrite	221

Table 4.3.5 XRD Spectra of bike chain

#### 4.3.6 Vickers Hardness Test Results:

Vickers Hardness test results of the sample Bike chain are given in the Table 4.3.6 The average hardness of steel material has been found to be 145 HV which is natural for ferritic steels

Serial No.	Load (in kgf)	Length of One Diagonal (d1mm)	Length other diagonal (d2 mm)	Average (d mm)	Hardness (VHN) kgf/mm <sup>2</sup>
1	30	0.44	0.44	0.383	251

Table:4.3.6 Vickers Hardness Test of bike chain

#### 4.4. Analysis of a spoke of a Bike

The specimen of the fifth test sample is spoke of a Bike shown in Fig - 4.4. The details of dimensions are given below

Sample name :spoke of a bike

Diameter:3.34(mm)



Fig:4.4. spoke of a bike

##### 4.4.1 Source

This spoke of a Bike was collected

##### 4.4.2 Chemical Composition:

The chemical composition of the sample is given in Table 4.4.2 and was determined by spectroscopy method. The sample is a medium carbon steel of grade IS 1875/1992 SAE 1040

Elements	Value	Elements	Value	Elements	Value	Elements	Value
<b>C %</b>	0.351	Cu %	0.017	Ni %	0.034	Mo %	0.032
<b>Si %</b>	0.174	Al %	0.012	As %	>0.106	B %	0.002
<b>Mn %</b>	0.623	Sn %	00	Zr %	0.004	Nb %	<0.001
<b>P %</b>	0.036	Ti %	0.001	Co %	0.006	Pb %	00
<b>S %</b>	0.032	V %	0.007	Fe %	98.273	Sb %	00
<b>Cr %</b>	0.041	W %	<0.017	N %	00	Ta %	>0.042

Table:4.4.2 Chemical Composition of a spoke of a bike



### **4.4.3 Optical Microscopy**

The revealed microstructure in Fig 4.4.3. Shows ferrite and Pearlite almost in equal proportion.

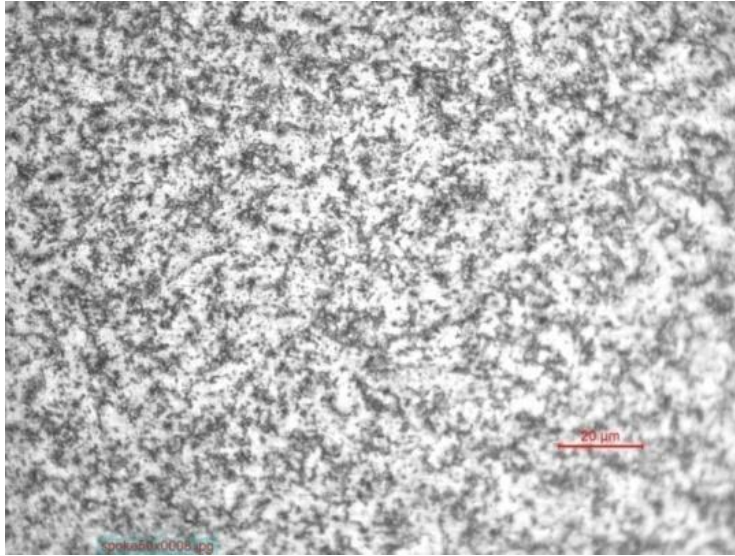


Fig. 4.4.3:[100 X Etchant-2% nital ]the microstructure shows the ferrite and pearlite.

### **4.4.4 SEM ANALYSIS:**

The SEM images of spoke of bike has been presented in the following Figures.4.4.4.a and fig 4.4.4.b .

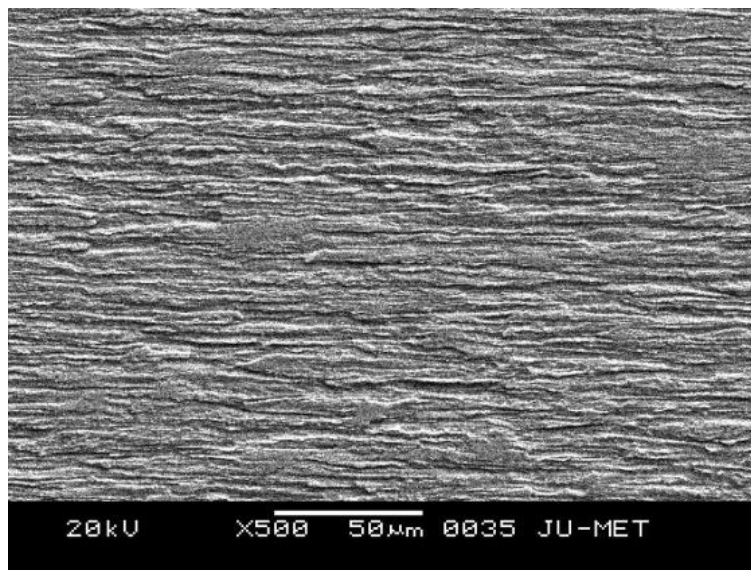


Fig. 4.4.4.a:[500 X Etchant-2% nital ] Rolling texture is quite apparent in the SEM image

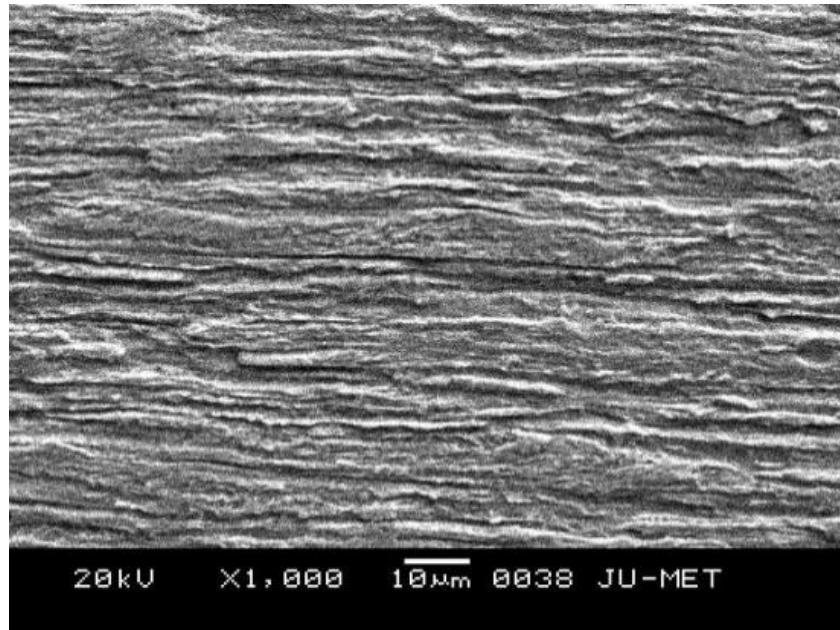


Fig. 4.4.4.b:[1000 X Etchant-2% nital ] Banded structure of pearlite has been revealed

#### 4.4.5 PHASE ANALYSIS BY XRD:

The X-Ray diffraction pattern on the spoke of a bike has been given in the Fig 4.4.5 and Table 4.4.5. Comparing with the JCPDS file ferrite phase is confirmed

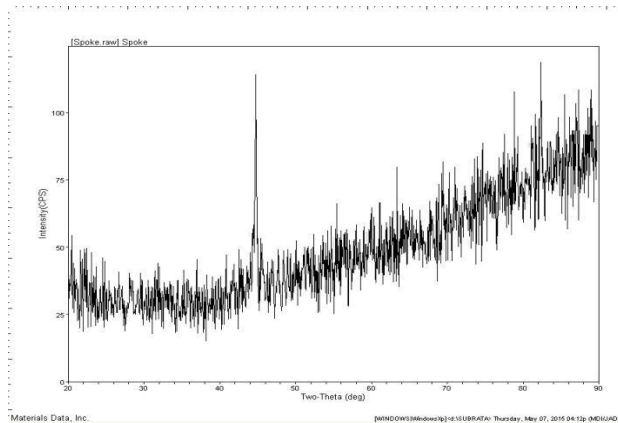


Fig:4.4.5 XRD Spectra of a spoke of a bike

Peak No.	2θ	d(A)	Intensity	Relative Intensity(I/I <sub>0</sub> )	Identified Phase	Diffracting Plane(hkl)
1	44.75	2.023	114	96	α-ferrite	(110)
2	78.85	1.212	108	91	Pearlite	(140)
3	87.35	1.169	119	100	α-ferrite	(322)

Table :4.4.5 XRD Spectra of a spoke of a bike

#### 4.4.6 Vickers Hardness Test Results:

Vickers Hardness test (Macro) results on the sample are given in the table 4.5.6. The hardness of steel material has been found to be 289.6 HV.

Serial No.	Load (in kgf)	Length of One Diagonal (d1 mm)	Length of the other diagonal (d2 mm)	Average (d mm)	Hardness (VHN)kgf/m <sup>2</sup>
1	30	0.253	0.253	0.253	289.65

Table:4.4.6 Vickers Hardness Test of spoke of a bike

#### 4.5. Clutch of a bike

The specimen of the Clutch of bodyis shown in Fig 4.5 .

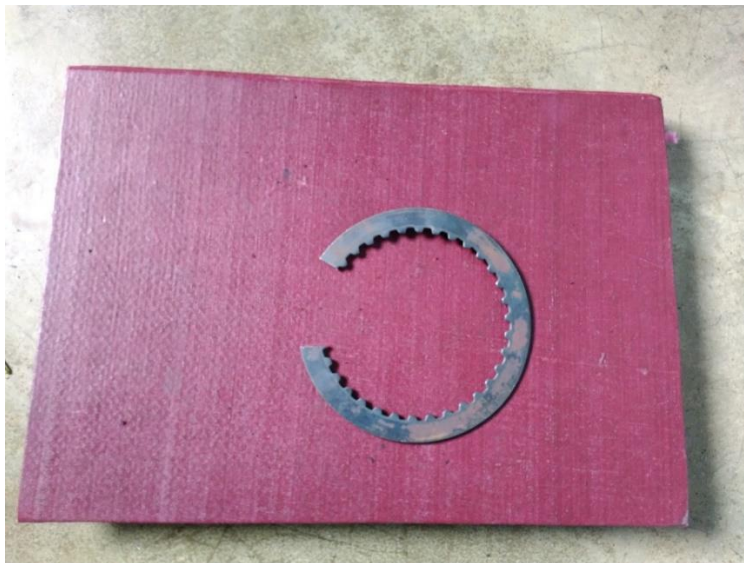


Fig: 4.5 Clutch of a bike

##### 4.5.1 Source

This clutch of a bike was obtained from a bike manufacturing unit.

##### 4.5.2Chemical Composition:

The chemical composition of Car Body Sheet is enlisted in Table 4.5.2. The amount of C

(0.0627% ) in the steel is very less comes under extra low C steels. This contains S (0.0104 %) p(0.0143)within industrial limit.

<b>Element</b>	<b>Value</b>	<b>Element</b>	<b>Value</b>	<b>Element</b>	<b>Value</b>	<b>Element</b>	<b>Value</b>
<b>C %</b>	0.063	<b>Cu %</b>	0.0967	<b>Bi %</b>	0.0464	<b>Mo %</b>	<0.000
<b>Si %</b>	0.032	<b>Al %</b>	0.0334	<b>Ca %</b>	0.0028	<b>B %</b>	<0.000
<b>Mn %</b>	0.253	<b>Sn %</b>	<0.000	<b>Ce %</b>		<b>Nb %</b>	0.0057
<b>P %</b>	0.014	<b>Ti %</b>	0.0005	<b>Co %</b>	0.0007	<b>Pb %</b>	0.0030
<b>S %</b>	0.010	<b>V %</b>	<0.004	<b>Fe %</b>	99.4	<b>Sb %</b>	<0.002
<b>Cr %</b>	0.030	<b>W %</b>	0.0097	<b>La %</b>	0.0059	<b>Ta %</b>	<0.010
<b>Ni %</b>	0.011	<b>As %</b>	<0.000	<b>N %</b>	0.0141	<b>Zr %</b>	0.0021

Table:4.5.2 Chemical composition of clutch of a bike

### 4.5.3 Optical Microscopy

The microstructures clutch of a bike are given in Fig 4.5.3.a and 4.5.3.b . The microstructures revealed ferrite grains with a lot of inclusions.

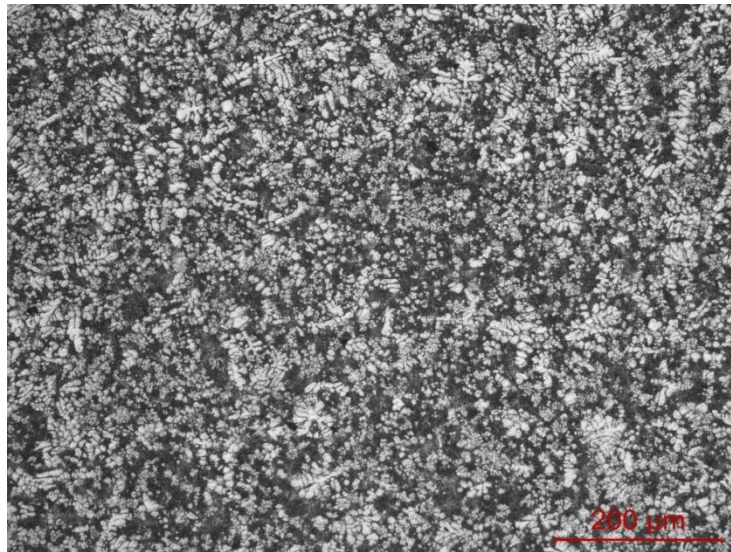


Fig. 4.5.3.a:[50X Etchant-2% nital ] The white regions are ferrite.

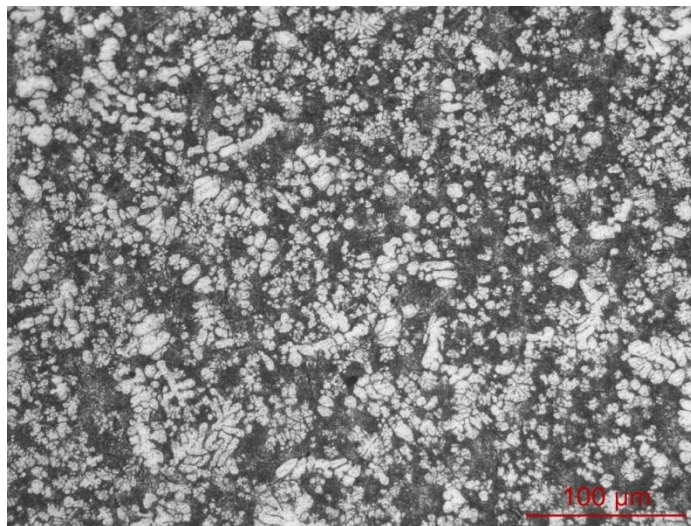


Fig. 4.5.3.b:[100X Etchant-2% nital ] The microstructure of cross section clearly indicates ferrite grains and the rolling direction.

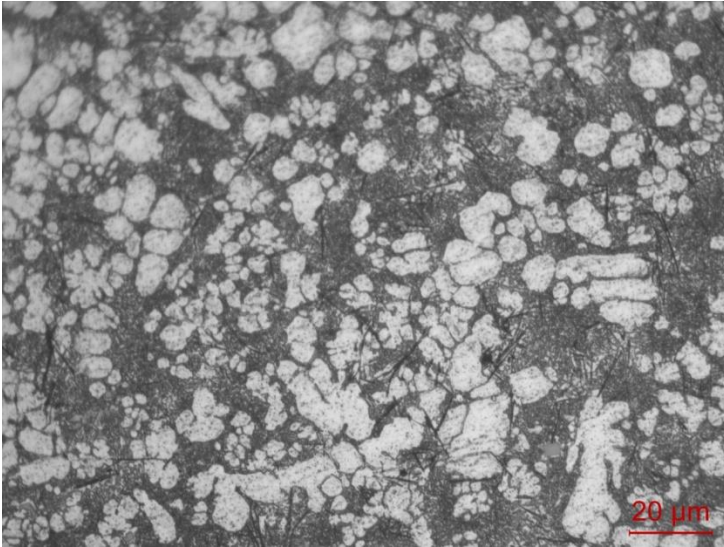


Fig. 4.5.3.c:[200X Etchant-2% nital ] The microstructure of cross section clearly indicates ferrite grains and the rolling direction

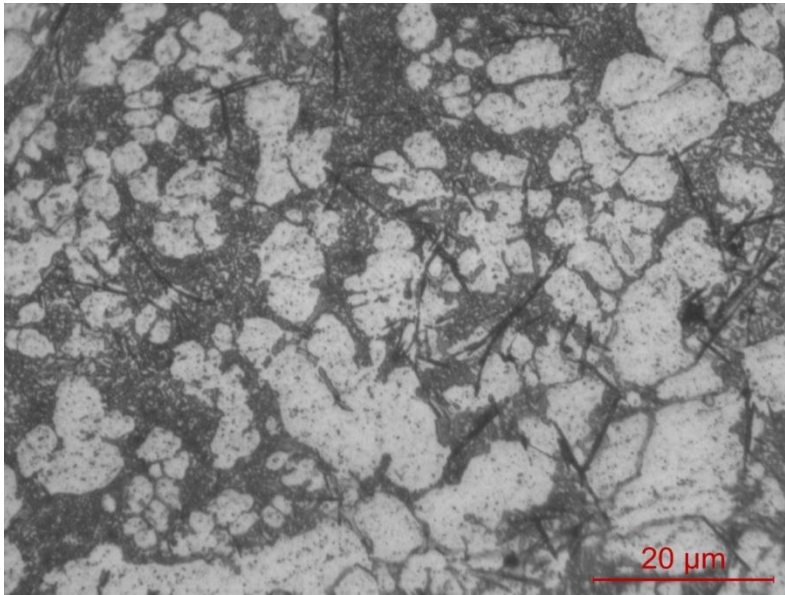


Fig. 4.5.3:d[500X Etchant-2% nital ]

#### 4.5.4 SEM ANALYSIS:

The SEM images of clutch of a bike has been presented in the Fig 4.5.4.a and 4.5.4.b. Equi-axed ferrite grains are visible.

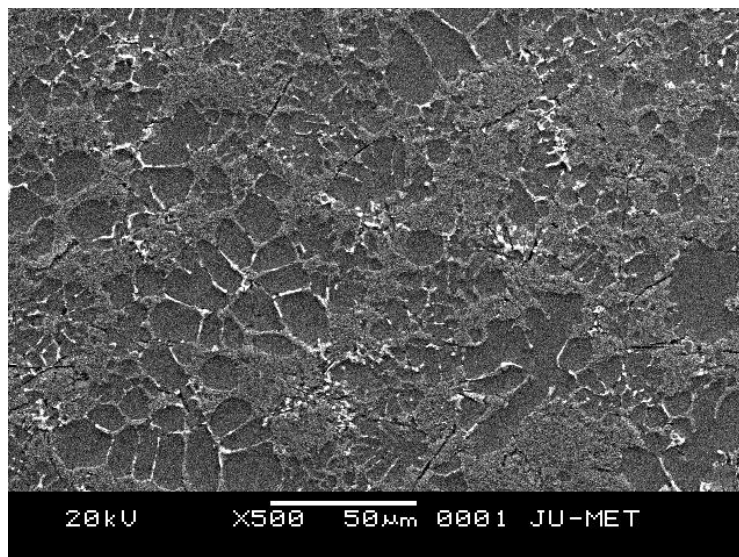


Fig. 4.5 .4:[500 X Etchant-2% nital ].



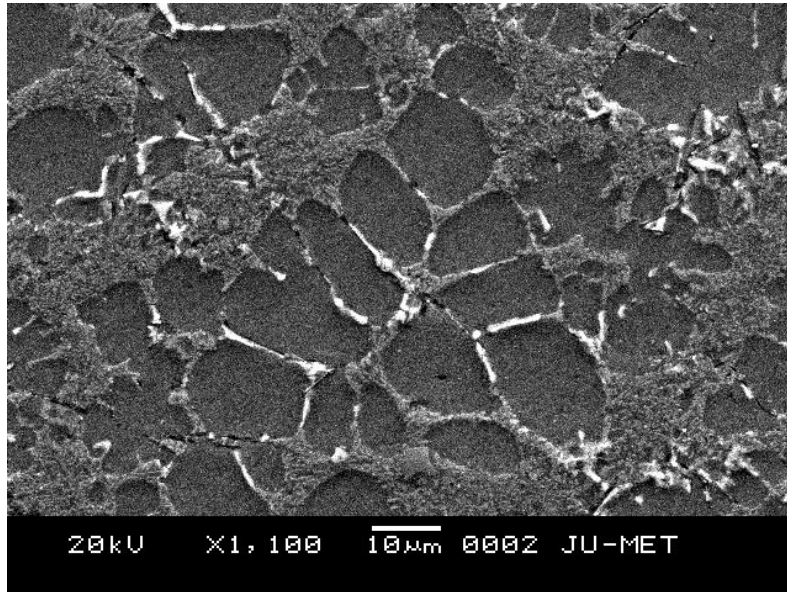


Fig. 4.5.4.b:[1000 X Etchant-2% nital ]. The grain boundaries had become prominent

#### 4.5.5 PHASE ANALYSIS BY XRD:

The X-Ray diffraction pattern on the clutch of a bike sample has been given in the Fig 4.5.5 and Table 4.5.3. Comparing with the JCPDS file ferrite phase is confirmed.

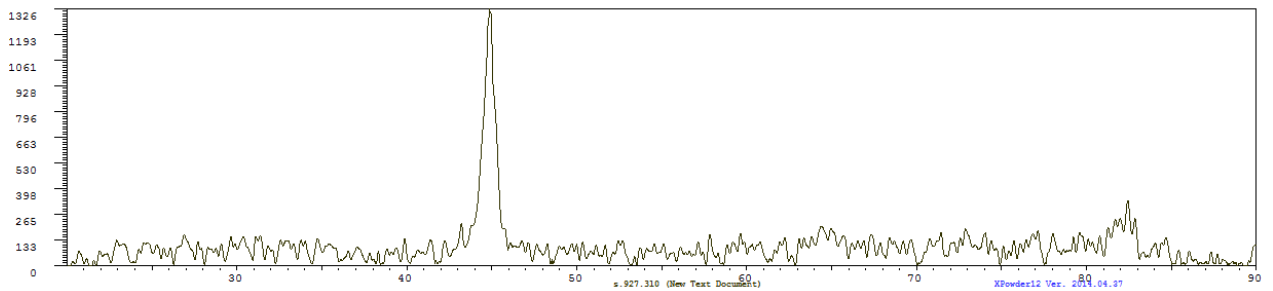


Fig:4.5.5 X- Ray Diffractogram of Clutch of a bike

Peak No.	2θ	d(A)	Intensity	Relative Intensity (I/I <sub>0</sub> )	Identified Phase	Diffracting Plane(hkl)
1	39.28	2.297	6430	100	α-ferrite	(110)
2	45.480	1.9926	3507	55	α-ferrite	(200)
3	65.800	1.418	3136	50	α-ferrite	(211)

Table:4.5.5 X- Ray Diffractogram of Clutch of a bike

#### 4.5.6 Vickers Hardness Test Results:

Vickers Hardness test results on the sample are given in the table 4.8.5.

Serial No.	Load (in kgf)	Length of One Diagonal (d1 mm)	Length of the other diagonal (d2 mm)	Average (d mm)	Hardness (VHN)kgf/m <sup>2</sup>
1	30	0.44	0.45	0.44	92.4

Table:4.5.6 Vickers Hardness Test of clutch

The of steel material has been found to be 92.4 HV.

## 5. GENERAL DISCUSSION

The sample of Kick Rod steel is low Carbon steel having around 0.189% carbon .The micro-structure reveals major ferrite phase with pearlite. Some inclusions are identified at higher magnifications. Some pores are also visible in the microstructure. XRD results also confirm presence of ferrite as a major phase and cementite association in pearlite grains. As expected, the hardness and yield strength were quite high. The Vickers hardness number is 156 kgf/mm<sup>2</sup> .yield strength of the sample is 326 N/mm<sup>2</sup>. The Carbon equivalent suggests non weldable property though it is not generally required in the product.

The sample lever arm of a bike is low Carbon steel having around 0.238% carbon The micro structure of the steel has fine pearlite as well as some  $\alpha$ -ferrite to strengthen the material for absorbing sock loading. XRD results also confirm presence of ferrite as a major phase and cementite association in pearlite grains. As expected, the hardness was high. The Vickers hardness number is 178.3 kgf/mm<sup>2</sup> .The Carbon equivalent suggests non weld able property though it is not generally required in the product. The low alloy Ni-Cr Steel has been used in the lever arm of the two wheeler for its excellent forging quality and high toughness. The micro structure of the steel has fine pearlite as well as some  $\alpha$ -ferrite to strengthen the material for absorbing sock loading.

The sample Bike chain was found to be of mild carbon category with some metal inclusion in well control to make it a clean grade of steel. The microstructure depicts  $\alpha$ -ferrite and cementite grains of equi-axed nature with some amount of inclusions. Both XRD and hardness also pointed towards ferritic nature .Some porosity are also visible .the size of porosity is big in this case.The hardness of the chain is quit high because of 0.370% of carbon results increase amount of pearlte.The hardness is 251 kgf/mm<sup>2</sup>.But presence of large porosity is present in the structure which may results in failure.

The sample of spoke of a bike is medium carbon steel having around 0.351% carbon containing. The micro structure of the steel has  $\alpha$ -ferrite with pearlite to strengthen the material for absorbing shock loading. All the SEM micrograph indicates presence ferrite & pearlite. The product seems to be rolled and platelets fibrous structure is formed. The XRD results also confirm presence of  $\alpha$ - ferrite as a major association in pearlite grains. The micro-structure reveals ferrite and pearlite almost in equal proportion. XRD results also confirm presence of ferrite. As expected, the hardness was very high. The Vickers hardness number is 289.65 kgf/mm<sup>2</sup> .Due to because of containing high percentage of carbon.The alloy Steel has been used as chain of two wheeler for its excellent rolling and forging quality and high toughness.

The sample Clutch of a bike was found to be of extra low carbon category in well control to make it a clean grade of steel. The microstructure depicts ferrite grains with some amount of inclusions. Both XRD and hardness also pointed towards ferritic nature .The amount of carbon of the sample is .063 which is quit low. As carbon contain is low so Vickers hardness number is low which is 92.4 kgf/mm<sup>2</sup>.Ferrites being the bulk phase the steels performs soft and ductile, and are hugely appreciated by engineers in commercial operations for excellent formability

All the steel samples and the sole ductile iron sample show very rigorous processing technology of quality metals.The cause behind the bulk ferrite structure obviously belong to low or in few cases very low carbon .The hard ness of low carbon steel is low.Steel samples being used in transport section are naturally subjected to fatigue environment. To address the problems forging as well as heat treatment were practiced.The application of all these principles of hot processing and controlled cooling of ferrite at designated rates has been executed by modern steel maker known as TMCP (thermo-mechanical controlled processing)

Clean steel production was attempted by producers but not always the quality of the materials was uniform. However, in view of limited experiments and small batch of samples tested, no sweeping comments can be made. More studies and testing should be tried to resolve final assessment of the materials.

**CHAPTER 5**  
**REFERENCE**

## REFERENCE

1. Brady, George S.; Clauser, Henry R.; Vaccari A., John (1997). *Materials Handbook* (14th Ed.). New York, NY: McGraw-Hill. ISBN 0-07-007084-9.
2. *ibid.* pp 301 – 303.
3. *ibid.* pp 269 – 270.
4. *ibid.* pp 270 – 273.
5. Rollason, E.C., *Metallurgy for Engineers*, The English Language Book Society and Edward Arnold Publishers Limited, Third Edition (1961), pp 179 – 181.
6. Gupta, C.K., Suri A.K, *Ferro Alloys Technology in India*, Milind Publications Private Limited, (1982), p 36.
7. *ibid.* pp 44 – 47.
8. Lonsdale, C.P., *Thermit Rail Welding: History, Process Developments, Current Practices and Outlook for the 21<sup>st</sup> Century*, pp 3 – 5.
9. Dieter, G.E., *Mechanical Metallurgy*, McGraw- Hill Book Company, pp 503 – 505.
10. Eurocode 3: 'Design of Steel Structures' ENV 1993-1-1: Part 1.1: General Rules and Rules for Buildings, CEN, 1992.
11. Llewellyn, D.T., Hudd, R.C., *Steels Metallurgy and Applications*, Third Edition, (1998), pp 19 – 23.
12. *Materials Transactions*, Vol. 50, No. 8 (2009) pp. 1919 to 1923 #2009 The Japan Institute of Metals

13. J. R. Kremer, D. N. Mastronarde and J. R. McIntosh: *J. Struct. Biol.* 116 (1996) 71–76.
14. Material Science and Metallurgy, Part II, Course C9, Alloys, H.K.D.H. Bhadeshia.
15. *Journal of High Temperature Society*, Volume 31, Issue 4, pp. 239-244 (2007).
16. Hsu, C.H., Material Science and Engineering Laboratory, California State University, (2005), pp 9 – 10.
17. Cullity, B.D., *Elements of X-Ray Diffraction*, Addison-Wesley, (1978), pp 398 – 403.
18. C. Chen, *Magnetism and Metallurgy of soft magnetic materials*. North Holland, 1977.
19. Fink and Beaty, *Standard Handbook for Electrical Engineers 11th Edition*, pages 17–19.
20. "Forging Shapes". All Metals & Forge Group. Retrieved 1 October 2013.
21. SAIL HAND-BOOK 2014.



## **Websites**

1. [http://www.most.gov.mm/techuni/media/Met04033\\_52\\_121.pdf](http://www.most.gov.mm/techuni/media/Met04033_52_121.pdf)
2. <http://courses.washington.edu/mse170/powerpoint/Zhang/19.pdf>
3. <http://www.new.manufacturinget.com/p=578>
4. <http://www.gowelding.com/met/carbon.htm>
5. [www.substech.com](http://www.substech.com)